Robust Design of Multi-Energy Systems Accounting for Mixed-Integer Operational Problems

Moritz Wedemeyer[a,b], Alexander Mitsos[d,a,c], Manuel Dahmen[a,*]

[a] Institute of Climate and Energy Systems, Energy Systems Engineering (ICE-1), Forschungszentrum Jülich GmbH, Jülich 52425, Germany

[b] RWTH Aachen University, Aachen 52062, Germany

[c] RWTH Aachen University, Process Systems Engineering (AVT.SVT), Aachen 52074, Germany

[d] JARA-ENERGY, Jülich 52425, Germany

Identifying robust designs for multi-energy systems is computationally challenging. As rigorous approaches are often computationally intractable, heuristics are employed to generate candidate designs. One example is the feasibility time-step heuristic by Teichgraeber et al. [Appl. Energy, 275, 115223, 2020]. We theoretically investigate how three common nonconvexities, i.e., piecewise-linear energy inflow-outflow relationships, minimal part-loads, and storage complementarity, affect the robustness of designs identified by this heuristic. We find that, if surplus energy cannot be curtailed, any of these nonconvexities may cause the heuristic to fail. If curtailment is allowed, storage complementarity does not compromise robustness, and convex piecewise-linear inflow-outflow relationships can be reformulated linearly. However, minimal part loads may lead to failure of the heuristic. Furthermore, if the objective function of the operational problem is not jointly convex in the uncertain variables and the operational variables, the heuristic may fail. We consider an illustrative multi-energy system, where minimal part-loads and nonconvex dependence of the objective function on heat-pump efficiency are identified as possible failure modes. We propose a hybrid method that discretizes integer variables and embeds the dual of the lower-level problem into a single-level formulation to verify whether a design identified by the heuristic is robust. The results show that the feasibility time-step heuristic may identify robust designs despite the presence of nonconvexities, but the success is case-dependent. Hence, the heuristic can serve as a first step in identifying robust designs; however, when robustness guarantees are required, rigorous methods are necessary.

Keywords: *Robust optimization, Multi-energy systems, Robust energy system design, Mixed-integer linear programming*

*M. Dahmen, Institute of Climate and Energy Systems, Energy Systems Engineering (ICE-1), Forschungszentrum Jülich GmbH, Jülich 52425, Germany
E-mail: m.dahmen@fz-juelich.de

1 Introduction

When designing multi-energy systems, it is paramount that these are robust, i.e., they can meet any energy demand that the system is expected to encounter during operation. Robustness is an even stronger concern in isolated energy systems, which are not connected to a superordinate grid. The limited number of users and small geographic extent of isolated systems lead to large relative fluctuations in load and renewable generation, necessitating robustness against uncertainties in both demand and renewable supply. To hedge against uncertainty, multi-energy systems are often designed using historical realizations of the uncertainties. As incorporating the full historical dataset is often computationally intractable, time-series aggregation methods are frequently applied (Kotzur et al., 2018; Teichgraeber and Brandt, 2019; Fleschutz et al., 2025).

A major limitation of these aggregation approaches is that they often neglect extreme events, even though such events can strongly influence system costs (Bahl et al., 2017a). Consequently, several approaches have been developed to better account for extreme scenarios. One option is to manually include extreme periods in the representative scenarios used for system design (Domínguez-Muñoz et al., 2011; Voll et al., 2013). In a similar vein, Gabrielli et al. (2019) created synthetic worst-case scenarios with artificially increased demands and analyzed the robustness of the candidate designs. However, the interactions between different uncertainties are difficult to assess a priori.

In a series of papers, Bardow and co-workers (Bahl et al., 2017a, 2018; Baumgärtner et al., 2019a,b) developed methods that iteratively refine the temporal resolution of aggregated time series to accurately approximate the optimal objective value of the full dataset for mixed-integer linear programming (MILP) energy system design problems. Wang et al. (2024) extended these methods to nonlinear problems. In addition to improving the approximation of system costs, these approaches also aim to ensure the feasibility of the candidate design for the complete historical dataset. In a similar vein, Teichgraeber et al. (2020) introduced the feasibility time-step heuristic, based on work by Bahl et al. (2017b). Instead of increasing the resolution of the entire time series, as done in Bahl et al. (2017a, 2018); Baumgärtner et al. (2019a,b), Teichgraeber et al. (2020) and Bahl et al. (2017b) iteratively check the operational problem for feasibility, and add violating scenarios to the design problem.

However, feasibility with respect to the historical data alone may not be sufficient to guarantee feasibility for future uncertainty realizations (Wedemeyer et al., 2026), since the available historical data represent only a finite subset of all possible operating conditions. To obtain robustness guarantees, robust optimization (Ben-Tal et al., 2009), originally introduced by Soyster (1973), can be employed. Robust optimization addresses optimization problems with uncertain parameters, e.g., future energy demands,

renewable generation, and energy prices. The objective is to identify solutions that remain feasible for all realizations of the uncertain parameters within a predefined uncertainty set. Enforcing feasibility for all possible uncertainty realizations naturally leads to semi-infinite programs (SIPs) (Stein, 2003; Charnes et al., 1962), which involve finitely many decision variables but infinitely many constraints.

In many energy system applications, some decisions must be taken before the uncertainty is realized, while others can be adjusted afterwards. This setting is commonly addressed using adjustable robust optimization (Ben-Tal et al., 2004), in which here-and-now decisions are complemented by wait-and-see variables acting as recourse decisions. Including recourse decisions leads to multi-level optimization problems, making adjustable robust optimization problems even harder to solve than regular robust optimization problems.

Existing approaches, therefore, typically balance the tractability of the robust optimization problem against the generality of the uncertainty set and the flexibility of the recourse decisions. Majewski et al. (2017) proposed a robust energy system design approach, but restricted the uncertainty set to intervals around nominal parameter values. They reformulated the resulting SIP into a tractable single-level problem by considering only the extreme values of these intervals. However, Grossmann and Sargent (1978) have shown that this reformulation is not valid for general polyhedral uncertainty sets. Similarly, Abdin et al. (2022) propose an adjustable robust optimization approach based on the same interval-type uncertainty set, in which wait-and-see variables are approximated using affine decision rules parametrized by here-and-now variables. In contrast, Shen et al. (2020) introduce a data-driven uncertainty set to better capture the correlation between uncertain parameters, but do not explicitly model recourse decisions.

Recently, we transferred a robust design approach from process systems engineering (Grossmann and Sargent, 1978) to energy system design (Wedemeyer et al., 2026). While this approach enables the exact solution of robust energy system design problems without restrictions on the structure of the uncertainty set or the recourse decisions, it is computationally demanding. Consequently, in practical settings, heuristics such as the feasibility time-step heuristic (Teichgraeber et al., 2020) may still be needed.

We previously proved that for convex operational problems, the feasibility time-step heuristic (Teichgraeber et al., 2020) indeed guarantees feasibility for all scenarios within the convex hull of the historical data (Wedemeyer et al., 2026). However, multi-energy system design problems are often formulated as MILP problems, which are inherently nonconvex (Ommen et al., 2014; Kotzur et al., 2021; Wirtz et al., 2021; Hoffmann et al., 2024; Mancò et al., 2024). As a result, the robustness guarantees established for convex operational problems no longer apply. Nevertheless, already the original work by Bahl et al.

(2017b) applied the heuristic to an MILP energy system synthesis problem.

This raises the question of whether practically relevant nonconvexities invalidate the robustness guarantees of the heuristic. In our previous work (Wedemeyer et al., 2026), we showed that minimal part load operation, if combined with a no-curtailment assumption, can cause the feasibility time-step heuristic (Teichgraeber et al., 2020) to identify designs which are not robust, i.e., for which not all realizations in the uncertainty set are feasible. However, the example was minimal, considered only a single timestep, and relied on the assumption that surplus energy could not be curtailed.

In the present work, we extend this analysis and provide comprehensive guidelines for assessing the robustness of designs obtained using the feasibility time-step heuristic. Specifically, we (i) classify common nonconvexities in multi-energy system models, (ii) analyze their impact on robustness, and (iii) propose a method to rigorously verify candidate designs. To the best of our knowledge, this is the first systematic analysis of how typical nonconvexities affect robustness and the first work to provide general guidelines for the robust application of the feasibility time-step heuristic. The findings, therefore, have important implications for the robust design of multi-energy systems with MILP operational problems.

The remainder of this work is structured as follows. Section 2 presents the modeling framework for multi-energy system design and discusses the key nonconvexities arising in the operational problem. Their impact on robustness is then analyzed. Section 3 introduces an illustrative case study that demonstrates the impact of nonconvexities. Additionally, a method is proposed to verify whether a design candidate is robust for all scenarios within the convex hull of the historical data, and its application is demonstrated using the case study. Finally, Section 4 discusses the results and summarizes the main findings.

2 Problem Structure

Throughout the manuscript, scalar-valued quantities are denoted in regular font, e.g., x, vector-valued quantities are denoted in bold font, e.g., $\mathbf{x}$, and set-valued quantities are denoted in calligraphic font, e.g., $\mathcal{X}$. We consider energy system design problems of the form:

$$\begin{aligned} \min_{\mathbf{x}\in\mathcal{X},\mathbf{z}_s\in\mathcal{Z}_s(\mathbf{x})\forall s\in\mathcal{S}} \quad & c_{inv}(\mathbf{x}) + \sum_{s\in\mathcal{S}} c_{op}(\mathbf{z}_s) \\ \text{s.t.} \quad \max_{\mathbf{y}\in\mathcal{Y}} \min_{\mathbf{z}\in\mathcal{Z}(\mathbf{x},\mathbf{y})} \quad & E_{gap}(\mathbf{x},\mathbf{y},\mathbf{z}) \leq 0 \end{aligned} \tag{PS}$$

with feasible sets

$$\mathcal{X} = \{\mathbf{x} \in \mathbb{R}^{n_x} |\ \mathbf{g}_x(\mathbf{x}) \leq \mathbf{0}\ (\textit{Design constraints})\}$$
$$\mathcal{Z}_s(\mathbf{x}) = \{\mathbf{z}_s \in \mathbb{R}^{n_z} |\ \mathbf{g}_{en}(\mathbf{x}, \mathbf{y}_s, \mathbf{z}_s) \leq \mathbf{0}\ (\textit{Energy system model})\}$$
$$\mathcal{Y} = \{\mathbf{y} \in \mathbb{R}^{n_y} |\ \mathbf{g}_y(\mathbf{y}) \leq \mathbf{0}\ (\textit{Uncertainty bounds})\}$$
$$\mathcal{Z}(\mathbf{x}, \mathbf{y}) = \{\mathbf{z} \in \mathbb{R}^{n_z} |\ \mathbf{g}_{en}(\mathbf{x}, \mathbf{y}, \mathbf{z}) \leq \mathbf{0}\ (\textit{Energy system model})\},$$

where $\mathbf{x}$ represents design decisions such as component capacities, $\mathbf{y}_s$ are the fixed uncertainty realizations of the representative scenarios s, and $\mathbf{z}_s$ represents the corresponding upper-level operational decisions such as component energy outflow. c_{inv} and c_{op} are the investement and operational costs, respectively. $\mathbf{g}_x(\mathbf{x})$ are the design constraints, e.g., piecewise-linear investment curves, and $\mathbf{g}_y(\mathbf{y})$ are the uncertainty bounds, i.e., constraints describing the convex hull of the historical data. $\mathbf{g}_{en}(\mathbf{x}, \cdot, \cdot) \leq \mathbf{0}$ are the model equations that describe the behavior of the energy system.

$$\max_{\mathbf{y} \in \mathcal{Y}} \min_{\mathbf{z} \in \mathcal{Z}(\mathbf{x}, \mathbf{y})} \quad E_{gap}(\mathbf{x}, \mathbf{y}, \mathbf{z}) \tag{MLP}$$

An embedded optimization problem, which we refer to as the medial-level problem (MLP), ensures the feasibility of the design for all possible uncertainty realizations $\mathbf{y}$, such as wind-power realizations, using operational recourse decisions $\mathbf{z}$ to counteract the uncertainty realization. We refer to the objective function of problem (MLP) as the energy gap, which is defined as:

$$E_{gap}(\mathbf{x}, \mathbf{y}, \mathbf{z}) = \max_{e \in \mathcal{E}, t \in \mathcal{T}} \left\{ \dot{E}_{e,dem,t} - \sum_{c \in \mathcal{C}_{e,out}} \dot{E}_{e,c,t} + \sum_{c \in \mathcal{C}_{e,in}} \dot{E}_{e,c,t} + \sum_{c \in \mathcal{C}_{e,sto}} \left(\dot{E}_{e,c,t,in} - \dot{E}_{e,c,t,out} \right) \right\} \tag{1}$$

Here, the energy gap represents the maximum energy balance violation across all energy forms $e \in \mathcal{E}$ and timesteps $t \in \mathcal{T}$. $\dot{E}_{e,dem,t}$ is the energy demand for energy form e at time t, and $\dot{E}_{e,c,t}$ represent energy flows associated with component c, where $\mathcal{C}_{e,in}$ and $\mathcal{C}_{e,out}$ denote the sets of components consuming and supplying energy form e, respectively. For storage components $c \in \mathcal{C}_{e,sto}$, $\dot{E}_{e,c,t,in}$ and $\dot{E}_{e,c,t,out}$ denote the energy inflows and outflows.

(PS) is a so-called existence-constrained semi-infinite program (ESIP) (Djelassi and Mitsos, 2021). Importantly, if the feasible set of the lower-level problem $\mathcal{Z}(\mathbf{x}, \mathbf{y})$ depends on the uncertain variables $\mathbf{y}$, (MLP) is a generalized semi-infinite program (GSIP). To facilitate the solution of (MLP), the coupling

constraints $g_j(\mathbf{y}, \mathbf{z})$ in $\mathcal{Z}(\mathbf{x}, \mathbf{y})$, which introduce the dependency of the medial-level variables $\mathbf{y}$, are moved into the objective function:

$$\max_{\mathbf{y}\in\mathcal{Y}} \min_{\mathbf{z}\in\mathcal{Z}(\mathbf{x})} \quad \max\left\{E_{gap}(\mathbf{x}, \mathbf{y}, \mathbf{z}), \max_{j\in\mathcal{J}}\{g_j(\mathbf{y}, \mathbf{z})\}\right\} \tag{MLP-ref}$$

Here $j \in \mathcal{J}$ are the indices of the coupling constraints. If (MLP) is replaced by (MLP-ref) in (PS), an equivalent ESIP is obtained (cf. Section 5.2.4 in Djelassi (2020)).

If $\mathcal{Y}$ is a polyhedral set, as we will assume here, a sufficient condition for the worst-case scenario to lie on a vertex of the uncertainty set is joint convexity of the optimal value function

$$\min_{\mathbf{z}\in\mathcal{Z}(\mathbf{x})} \quad \max\left\{E_{gap}(\mathbf{x}, \mathbf{y}, \mathbf{z}), \max_{j\in\mathcal{J}}\{g_j(\mathbf{y}, \mathbf{z})\}\right\}$$

with respect to $\mathbf{y}$ and $\mathbf{z}$ (Halemane and Grossmann, 1983). Consequently, if the objective function of the lower-level problem is not jointly convex in the uncertain variables or if there are nonconvexities in the operational problem, the worst-case scenario may not lie on a vertex of the uncertainty set, which may lead to failure of the feasibility time-step heuristic and thus a non-robust design (Wedemeyer et al., 2026).

(PS) can be solved using adaptive discretization approaches (Djelassi, 2020) based on the algorithm by Blankenship and Falk (1976). As shown in our previous work (Wedemeyer et al., 2026), these adaptive-discretization approaches are working in a similar principle as the feasibility time-step heuristic, which is illustrated in Figure 1. In both methods, design optimization is performed using a set of representative scenarios $\mathcal{S}$ drawn from the historical dataset $\mathcal{D}$ to obtain candidate designs. Subsequently, worst-case scenarios are iteratively identified and added to $\mathcal{S}$ to refine the design problem.

The two approaches differ in how the worst-case scenarios are determined. In the feasibility time-step heuristic, operational feasibility is evaluated for all historical scenarios. If one or more infeasible scenarios are identified, they are added to the representative scenario set, and a new candidate design is computed (cf. Figure 1). The procedure terminates once all historical scenarios are feasible, at which point the design is deemed robust with respect to the historical data.

In contrast, adaptive discretization algorithms (Djelassi, 2020) identify worst-case scenarios by solving (MLP-ref) directly. Consequently, if the uncertainty set $\mathcal{Y}$ is defined as the convex hull of the historical data, the feasibility time-step heuristic solves a relaxation of (PS) (Wedemeyer et al., 2026).

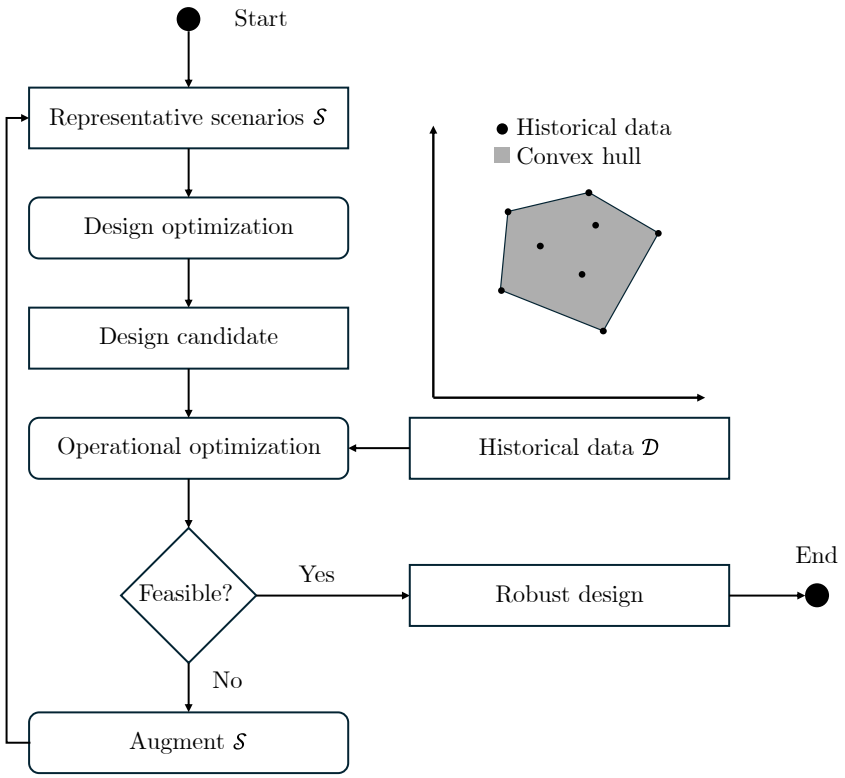

Fig. 1. Illustration of the feasibility time-step heuristic (Teichgraeber et al., 2020): A candidate design is obtained using a set of representative scenarios $\mathcal{S}$. Its operational feasibility is evaluated for all historical scenarios (circles) in the historical data $\mathcal{D}$. If all scenarios are feasible, the design is deemed robust; otherwise, the set of representative scenarios is augmented with one or more infeasible scenarios from the historical data, and the procedure is repeated. For convex operational problems, the feasibility of all historical scenarios guarantees feasibility for the entire interior of their convex hull (shaded region) (Wedemeyer et al., 2026).

2.1 Common nonconvexities

Looking at recent publications and reviews of energy system modeling (Ommen et al., 2014; Kotzur et al., 2021; Wirtz et al., 2021; Hoffmann et al., 2024; Mancò et al., 2024), we have identified 5 types to which nonconvexities occurring in energy system design problems can typically be attributed:

1. Piecewise-linear investment curves
2. Multiple units of the same component type
3. Piecewise-linear performance curves
4. Minimal part-loads
5. Complementarity of storage input and output

In this work, we focus on the impact of nonconvexities on the robustness of energy system designs. Piecewise-linear investment curves and integer variables used to model multiple units of the same component type appear only in the upper-level design problem (PS) and not in the embedded problem (MLP), which ensures the robustness of the design. Consequently, these nonconvexities do not affect the robustness of designs identified by the feasibility time-step method.

This leaves 3 relevant nonconvexities in the operational problem. For these nonconvexities, their impact depends on two additional factors: (i) whether the input energy flow of the considered component is externally supplied, and (ii) whether curtailment of excess energy is permitted. Multi-energy systems comprise components that convert between different energy carriers and must satisfy demand constraints for each carrier. If the input energy form is externally supplied and thus does not appear in any system balance equation, the nonconvexities affect only operational costs but not robustness, as the external supply is assumed to be able to meet any required demand. Curtailment refers to the ability to dispose of surplus energy, for example, by releasing excess heat to the environment via a heat exchanger. Curtailment has a substantial influence on the mathematical structure and difficulty of the problem. If curtailment is allowed, (PS) constitutes a regular ESIP (Djelassi and Mitsos, 2021), in which the objective function (1) of the medial-level problem (MLP) must be less than or equal to zero. If curtailment is prohibited, the energy balance must be satisfied exactly, resulting in a semi-infinite equality constraint. However, the presence of a semi-infinite equality constraint violates the assumption that a Slater point exists (Djelassi and Mitsos, 2021). The existence of Slater points, even near-optimal ones, is rather standard among deterministic global solution methods for semi-infinite problems, including for (PS), as they rely on restriction to generate feasible bounds (upper bounding procedure). In the absence of Slater points,

the algorithms, including those proposed in Djelassi and Mitsos (2021), are not guaranteed to converge, and typically do not do so in practice. In the presence of semi-infinite equality constraints, specialized solution strategies are required, e.g. Djelassi et al. (2019) or Stuber and Barton (2015). In line with previous works on the robustness of energy systems (Majewski et al., 2017), we focus on the case with curtailment, as it yields a more tractable yet realistic optimization problem formulation. In practice, excess energy can often be dissipated, e.g., via curtailing renewable energy sources or dissipating heat energy to the environment through the use of heat exchangers.

In addition to the previously mentioned nonconvexities in the operational problem, the way uncertainties enter the operational problem can also lead to the feasibility time-step heuristic being unable to identify a robust design. Typical uncertainties in energy system optimization problems include energy demand and weather realizations.

While energy demand enters the operational problem linearly in the energy balance equations of the objective function (1), weather variables may appear nonlinearly. For example, the efficiency of a heat pump $\eta_{hp,nom,t}(T_{amb,t})$ may depend on ambient temperature $T_{amb,t}$ (Sass et al., 2020) and appears in the energy inflow-outflow relation as:

$$\dot{E}_{e_{in},hp,t} - \frac{\dot{E}_{e_{out},hp,t}}{\eta_{hp,nom,t}(T_{amb,t})} = 0$$

When $\dot{E}_{e_{in},hp,t}$ is replaced in the energy balance by the expression $\frac{\dot{E}_{e_{out},hp,t}}{\eta_{hp,nom,t}(T_{amb},t)}$, a nonconvex dependency of the objective function (1) on the uncertain variable $\eta_{hp,nom,t}(T_{amb},t)$ arises.

Therefore, when assessing the validity of the feasibility time-step heuristic, it is necessary to consider not only the convexity of the operational problem but also whether the objective function (1) of the medial-level problem (MLP) is jointly convex in the uncertain variables $\mathbf{y}$ and the operational variables $\mathbf{z}$ (Halemane and Grossmann, 1983). The influence of the 3 relevant nonconvexities in the operational problem and the joint nonconvexity of the objective function on robustness is summarized in Table 1.

In the following sections, we will describe the 3 nonconvexities and under which conditions they may pose challenges to the feasibility time-step heuristic.

2.2 Piecewise-linear performance curves

Nonlinear component efficiency curves can be approximated using piecewise-linear functions. Rather than modeling the efficiency curves directly, it is often advantageous to describe the relationship between the energy inflow and outflow of a conversion component, as this relationship typically exhibits a more

linear behavior (Voll et al., 2013). The relevance of component performance curves in the context of robustness depends on whether the input energy carrier is externally supplied or must be provided by the multi-energy system itself. For example, meeting a cooling demand with a compression chiller induces an additional electricity demand within the system, whereas externally supplied inputs, such as natural gas for a boiler, are assumed to be unconstrained and affect only operational costs. Consequently, for robustness analysis, performance relations of components whose inputs are externally supplied can be replaced by admissible energy outflow ranges. In contrast, if a component induces additional demand for another energy carrier, the feasibility time-step heuristic may fail in providing a robust design.

The piecewise-linear relationship between the energy inflow and outflow of a conversion component $\dot{E}_{e_{in}}(\dot{E}_{e_{out}})$ can be modeled as follows according to Sass et al. (2020):

$$\dot{E}_{e_{in}} = \sum_{j \in \mathcal{J}} \left(b_j \lambda_{in,j} \frac{\dot{E}_{nom}}{\eta_{nom}} + \frac{\beta_j}{\eta_{nom}} \left(\dot{E}_{e_{out},j} - \lambda_{out,j} b_j \dot{E}_{nom} \right) \right)$$

$$\lambda_{out,j} \dot{E}_{nom} b_j \leq \dot{E}_{e_{out},j} \qquad \forall j \in \mathcal{J}$$

$$\lambda_{out,j+1} \dot{E}_{nom} b_j \geq \dot{E}_{e_{out},j} \qquad \forall j \in \mathcal{J}$$

$$\sum_{j \in \mathcal{J}} b_j = 1$$

$$\dot{E}_{e_{out}} = \sum_{j \in \mathcal{J}} \dot{E}_{e_{out},j}$$

Here, $\dot{E}_{e_{in}}$ and $\dot{E}_{e_{out}}$ denote the total energy inflow and outflow of the component, respectively, and $\dot{E}_{nom}$ is the nominal capacity of the component. The binary variable b_j selects the active segment $j \in \mathcal{J}$ of the piecewise-linear approximation. The parameters $\lambda_{in,j}$ and $\lambda_{out,j}$ define the breakpoints of the approximation, and the slope

$$\beta_j = \frac{\lambda_{in,j+1} - \lambda_{in,j}}{\lambda_{out,j+1} - \lambda_{out,j}}$$

characterizes segment j. The parameter η_{nom} denotes the nominal efficiency. This formulation represents a piecewise-linear approximation of the conversion efficiency. During design optimization, the bilinear terms $b_j \dot{E}_{nom}$ can be linearized using Glover's reformulation (Glover, 1975). In the operational problem, $\dot{E}_{nom}$ is a fixed parameter, and the formulation directly reduces to a linear model.

A simple multi-energy system with two energy forms, e_{in} and e_{out}, and allowed curtailment can be

represented by the following operational feasibility problem:

$$
\begin{aligned}
\min_{\mathbf{z}\in\mathcal{Z},\phi\in\mathbb{R}} \quad & \phi \\
s.t. \quad & \dot{E}_{e_{in},agg} + \dot{E}_{e_{in}} \leq \phi \\
& \dot{E}_{e_{out},agg} - \dot{E}_{e_{out}} \leq \phi \\
& \dot{E}_{e_{in}} = \sum_{j\in\mathcal{J}} b_j \lambda_{in,j} \frac{\dot{E}_{nom}}{\eta_{nom}} + \frac{\beta_j}{\eta_{nom}} \left(\dot{E}_{e_{out},j} - \lambda_{out,j} b_j \dot{E}_{nom} \right) \\
& \lambda_{out,j} \dot{E}_{nom} b_j \leq \dot{E}_{e_{out},j} && \forall j \in \mathcal{J} \\
& \lambda_{out,j+1} \dot{E}_{nom} b_j \geq \dot{E}_{e_{out},j} && \forall j \in \mathcal{J} \\
& \sum_{j\in\mathcal{J}} b_j = 1 \\
& \dot{E}_{e_{out}} = \sum_{j\in\mathcal{J}} \dot{E}_{e_{out},j}
\end{aligned}
$$

The component takes $\dot{E}_{e_{in}}$ as input energy and transforms it to $\dot{E}_{e_{out}}$, which it outputs, hence the opposite signs in the energy balance equations. ϕ is an auxiliary variable introduced to model the energy gap, i.e.,

$$E_{gap}(\mathbf{x},\mathbf{y},\mathbf{z}) = \max\{\dot{E}_{e_{in},agg} + \dot{E}_{e_{in}}, \dot{E}_{e_{out},agg} - \dot{E}_{e_{out}}\},$$

and the operation is feasible if $\phi \leq 0$. For simplicity, all other components and demands have been aggregated into $\dot{E}_{e_{in},agg}$ and $\dot{E}_{e_{out},agg}$, respectively, to focus solely on the influence of the piecewise-linear energy inflow-outflow.

Although many energy systems are modeled as MILP problems, the linearized performance curves are often convex and only appear nonconvex due to the modeling choice. For example, the piecewise-linear functions used by Voll (2014) to model the energy inflow-outflow relation of a boiler, a combined heat and power unit, an absorption chiller, and a compression chiller are all convex functions.

If the linearized energy inflow-outflow curve is convex, a simplified formulation of $\dot{E}_{e_{in}}(\dot{E}_{e_{out}})$ can be used (cf., Chapter 1.3 in Bertsimas and Tsitsiklis (1997) and Section 3.2.2 in Varelmann et al. (2022)):

$$\dot{E}_{e_{in}} = \max_{j\in\mathcal{J}} \left\{ b_j \lambda_{in,j} \frac{\dot{E}_{nom}}{\eta_{nom}} + \frac{\beta_j}{\eta_{nom}} \left(\dot{E}_{e_{out}} - \lambda_{out,j} b_j \dot{E}_{nom} \right) \right\}$$

This results in the following problem formulation by dropping the constraints describing the piecewise-

linear behavior in the general case:

$$
\begin{aligned}
\min_{\mathbf{z}\in\mathcal{Z},\phi\in\mathbb{R}} \quad & \phi \\
s.t. \quad & \dot{E}_{e_{in},agg} + \dot{E}_{e_{in}} \leq \phi \\
& \dot{E}_{e_{out},agg} - \dot{E}_{e_{out}} \leq \phi \\
& \dot{E}_{e_{in}} = \max_{j\in\mathcal{J}} \left\{ b_j \lambda_{in,j} \frac{\dot{E}_{nom}}{\eta_{nom}} + \frac{\beta_j}{\eta_{nom}} \left(\dot{E}_{e_{out}} - \lambda_{out,j} b_j \dot{E}_{nom} \right) \right\} \\
& \dot{E}_{e_{out}} \leq \dot{E}_{nom}
\end{aligned}
$$

By substituting, we obtain the inequality

$$
\dot{E}_{e_{in},agg} + \max_{j\in\mathcal{J}} \left\{ b_j \lambda_{in,j} \frac{\dot{E}_{nom}}{\eta_{nom}} + \frac{\beta_j}{\eta_{nom}} \left(\dot{E}_{e_{out}} - \lambda_{out,j} b_j \dot{E}_{nom} \right) \right\} \leq \phi,
$$

which can be formulated as multiple linear constraints (Bertsimas and Tsitsiklis, 1997; Varelmann et al., 2022):

$$
\dot{E}_{e_{in},agg} + b_j \lambda_{in,j} \frac{\dot{E}_{nom}}{\eta_{nom}} + \frac{\beta_j}{\eta_{nom}} \left(\dot{E}_{e_{out}} - \lambda_{out,j} b_j \dot{E}_{nom} \right) \leq \phi \quad \forall j \in \mathcal{J} \tag{2}
$$

Consequently, if the piecewise linearization of the energy inflow-outflow curve of the component is convex, i.e., $\dot{E}_{e_{in}}(\dot{E}_{e_{out}})$ is a convex function, it can be formulated fully linearly. As a result, the designs identified by the feasibility time-step heuristic are guaranteed to be robust.

In contrast, if the part-load behavior is nonconvex, this guarantee no longer holds; the feasibility time-step heuristic may still produce robust designs, but only incidentally. For clarity, we relabel the energy forms by 1 and 2 instead of using e_{in} and e_{out} since input and output energies differ across components.

An example of a system where the feasibility time-step heuristic fails can be written as follows:

$$
\begin{aligned}
&\min_{\mathbf{x}\in\mathcal{X},\mathbf{z}\in\mathcal{Z}} \dot{E}_{max,c_1} + \dot{E}_{max,c_2} \\
&s.t. \quad \dot{E}_{1,dem,d} + \dot{E}_{1,c_1,d} - \dot{E}_{1,c_2,d} \leq 0 && \forall d \in \mathcal{D} \\
&\quad \dot{E}_{2,dem,d} - \dot{E}_{2,c_1,d} \leq 0 && \forall d \in \mathcal{D} \\
&\quad \dot{E}_{1,c_1,d} = \sum_{j\in\mathcal{J}} b_{c_1,d,j}\lambda_{in,j}\frac{\dot{E}_{nom}}{\eta_{nom}} + \frac{\beta_j}{\eta_{nom}}\left(\dot{E}_{2,c_1,d,j} - \lambda_{out,j} b_{c_1,d,j}\dot{E}_{nom}\right) && \forall d \in \mathcal{D} \\
&\quad \lambda_{out,j}\dot{E}_{nom} b_{c_1,d,j} \leq \dot{E}_{2,c_1,d,j} && \forall d \in \mathcal{D}, \forall j \in \mathcal{J} \\
&\quad \lambda_{out,j+1}\dot{E}_{nom} b_{c_1,d,j} \geq \dot{E}_{2,c_1,d,j} && \forall d \in \mathcal{D}, \forall j \in \mathcal{J} \\
&\quad \sum_{j\in\mathcal{J}} b_{c_1,d,j} = 1 && \forall d \in \mathcal{D} \\
&\quad \dot{E}_{2,c_1,d} = \sum_{j\in\mathcal{J}} \dot{E}_{2,c_1,d,j} && \forall d \in \mathcal{D} \\
&\quad \dot{E}_{1,c_2,d} \leq \dot{E}_{max,c_2} && \forall d \in \mathcal{D} \\
&\quad \dot{E}_{2,c_1,d} \leq \dot{E}_{max,c_1} && \forall d \in \mathcal{D}
\end{aligned}
$$

with

$$
\begin{aligned}
&\mathbf{x} = [\dot{E}_{max,c_1}, \dot{E}_{max,c_2}] \\
&\mathcal{X} = \mathbb{R}^2_{\geq 0} \\
&\mathbf{z} = [\dot{E}_{1,c_1,1}, \ldots, \dot{E}_{1,c_1,|\mathcal{D}|}, \dot{E}_{2,c_1,1}, \ldots, \dot{E}_{2,c_1,|\mathcal{D}|}, \dot{E}_{1,c_2,1}, \ldots, \dot{E}_{1,c_2,|\mathcal{D}|}, \dot{E}_{2,c_1,1,1}, \ldots, \dot{E}_{2,c_1,|\mathcal{D}|,|\mathcal{J}|}, \\
&b_{c_1,1,1}, \ldots, b_{c_1,|\mathcal{D}|,|\mathcal{J}|}] \\
&\mathcal{Z} = \mathbb{R}^{|\mathcal{D}|(3+|\mathcal{J}|)}_{\geq 0} \times \{0,1\}^{|\mathcal{D}||\mathcal{J}|}
\end{aligned}
$$

Here, $\mathbf{x}$ are the design variables and $\mathbf{z}$ are operational variables. $\dot{E}_{max,c}$ are the component capacities, c_1 is a component with nonconvex $\dot{E}_1(\dot{E}_2)$ and c_2 is an externally supplied component that can supply $\dot{E}_1$, hence the input energy of c_2 does not occur in any of the energy balances. A schematic of the example system is shown in Figure 2 and the nonconvex piecewise-linear performance curve is illustrated in Figure 3. The operational constraints are enforced for every data point d in the historical data $\mathcal{D}$.

Figure 4 illustrates the historical data and the feasible region of the resulting design. Even though all three vertices of the convex hull are feasible, the convex hull contains infeasible regions. The infeasible

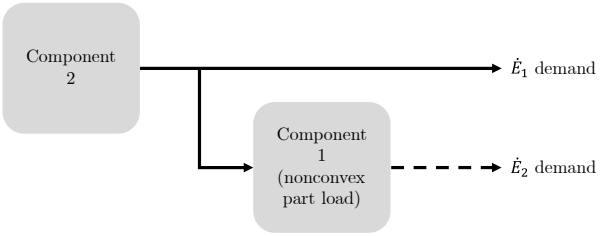

Fig. 2. Illustration of an example system with nonconvex part-load behavior for component 1. Component 2 is externally supplied and hence has no input energy here.

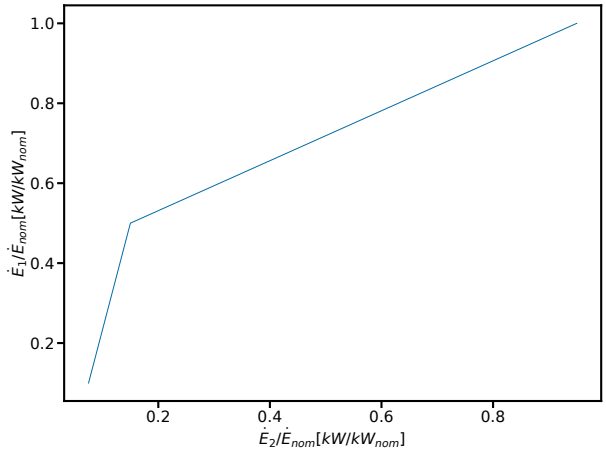

Fig. 3. Nonconvex piecewise-linear performance curve for Component c_1 in Figure 2.

region is approximated by sampling uniformly spaced energy demands and solving the corresponding operational feasibility problem. The worst-case scenario is identified by solving (MLP) using an adaptive discretization algorithm (Blankenship and Falk, 1976).

In the case where curtailment is not allowed, we have a semi-infinite equality constraint, which can be replaced by two corresponding inequality constraints, cf. Section 2.1, leading to the following *operational*

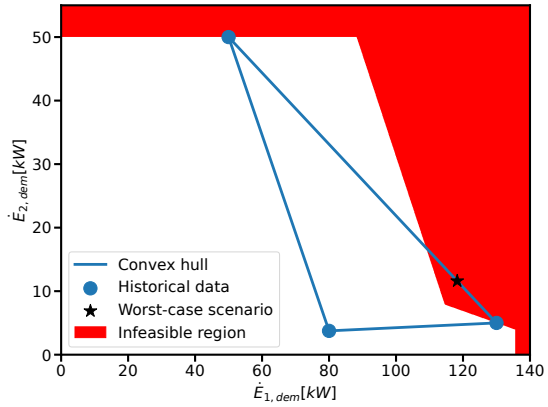

Fig. 4. Counter example that showcases how a design obtained using the feasibility time-step heuristic can fail to ensure feasibility within the convex hull of the historical data for a component with a nonconvex piecewise-linear energy inflow-outflow curve. The convex hull of historical demand data for energy forms 1 and 2 is plotted in blue. The infeasible region is shaded in red. The worst-case scenario inside the convex hull of the historical data is marked by a star. The example demonstrates that even if the heuristic identifies a design that is feasible for all historical scenarios, it may fail to guarantee feasibility for all points within the convex hull when nonconvexities are present.

feasibility problem:

$$
\begin{aligned}
\min_{\mathbf{z}\in\mathcal{Z},\phi\in\mathbb{R}} \quad & \phi \\
s.t. \quad & \dot{E}_{e_{in},agg} + \dot{E}_{e_{in}} \leq \phi \\
& \dot{E}_{e_{out},agg} - \dot{E}_{e_{out}} \leq \phi \\
& -\dot{E}_{e_{in},agg} - \dot{E}_{e_{in}} \leq \phi \\
& -\dot{E}_{e_{out},agg} + \dot{E}_{e_{out}} \leq \phi \\
& \dot{E}_{e_{in}} = \sum_{j\in\mathcal{J}} b_j \lambda_{in,j} \frac{\dot{E}_{nom}}{\eta_{nom}} + \frac{\beta_j}{\eta_{nom}} \left(\dot{E}_{e_{out},j} - \lambda_{out,j} b_j \dot{E}_{nom} \right) \\
& \lambda_{out,j} \dot{E}_{nom} b_j \leq \dot{E}_{e_{out},j} \qquad \forall j \in \mathcal{J} \\
& \lambda_{out,j+1} \dot{E}_{nom} b_j \geq \dot{E}_{e_{out},j} \qquad \forall j \in \mathcal{J} \\
& \sum_{j\in\mathcal{J}} b_j = 1 \\
& \dot{E}_{e_{out}} = \sum_{j\in\mathcal{J}} \dot{E}_{e_{out},j}
\end{aligned}
$$

Here, the inequalities with the opposite signs also appear:

$$E_{gap}(\mathbf{x},\mathbf{y},\mathbf{z}) = \max\{\dot{E}_{e_{in},agg} + \dot{E}_{e_{in}}, \dot{E}_{e_{out},agg} - \dot{E}_{e_{out}}, -\left(\dot{E}_{e_{in},agg} + \dot{E}_{e_{in}}\right), -\left(\dot{E}_{e_{out},agg} - \dot{E}_{e_{out}}\right)\}$$

Reformulation (2) used in the curtailment case is only applicable to constraints where the maximum term occurs with a positive sign (cf., Chapter 1.3 in Bertsimas and Tsitsiklis (1997)). $\dot{E}_{e_{in}}$, and hence the maximum term, occurs with a positive coefficient in one of the energy balances and with a negative coefficient in the complement of that energy balance, leading to the reformulation not being applicable in one case. Consequently, the feasibility time-step heuristic is not guaranteed to yield robust designs, even if the piecewise-linear performance curves themselves are convex.

2.3 Minimal part-load

Many energy conversion units have a minimal part-load requirement, below which they cannot operate, and binary variables are commonly used to model the on/off behavior of such components (Mancò et al., 2024):

$$\dot{E}_{e_{out}} \leq b\dot{E}_{max}$$
$$b\dot{E}_{min} \leq \dot{E}_{e_{out}}$$

Here, $\dot{E}_{e_{out}}$ is the energy outflow of the component, and $\dot{E}_{min}$ and $\dot{E}_{max}$ are the minimal and maximal energy outflows, respectively. If the binary variable $b = 0$, the component is off and $\dot{E}_{e_{out}} = 0$. If $b = 1$, the component is on, and the minimal part-load is enforced, i.e., $\dot{E}_{min} \leq \dot{E}_{e_{out}} \leq \dot{E}_{max}$. In our previous work (Wedemeyer et al., 2026), we demonstrated that when curtailment is not allowed, and the supplied energy outflow $\dot{E}_{e_{out}}$ must exactly meet the demand, minimal part-load constraints can render operation infeasible for low-demand scenarios.

However, if curtailment is allowed, the component can operate continuously at its minimal part-load, and any surplus energy can be dissipated. Similar to the case of piecewise-linear performance curves, minimal part-load constraints can be replaced by admissible energy outflow ranges if the energy inflow of the component is externally supplied and unconstrained, and hence cannot lead to the failure of the feasibility time-step heuristic. In contrast, if the energy inflow induces an additional demand in a different energy form within the multi-energy system, operating at minimal part-load may create an extra demand that cannot be satisfied, potentially leading to infeasibility. An example problem for which the feasibility time-step heuristic fails is shown in Figure 5. It consists of three components. Components 1 and 2 can

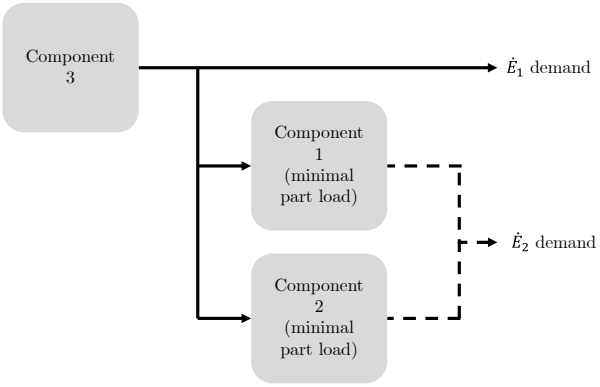

Fig. 5. Illustration of the minimal part-load example system.

convert energy form 1 into energy form 2, and component 3 can supply energy form 1 from an externally supplied energy form, which is not shown in the figure.

The corresponding design problem can be formulated as

$$
\begin{aligned}
\min_{\mathbf{x}\in\mathcal{X},\mathbf{z}\in\mathcal{Z}} \quad & \dot{E}_{max,c_1} + \dot{E}_{max,c_2} + \dot{E}_{max,c_3} \\
\text{s.t.} \quad & \dot{E}_{1,dem,d} + \dot{E}_{1,c_1,d} + \dot{E}_{1,c_2,d} - \dot{E}_{1,c_3,d} \leq 0 && \forall d \in \mathcal{D} \\
& \dot{E}_{2,dem,d} - \dot{E}_{2,c_1,d} - \dot{E}_{2,c_2,d} \leq 0 && \forall d \in \mathcal{D} \\
& \dot{E}_{1,c,d} = \dot{E}_{2,c,d} && \forall c \in \{c_1, c_2\} \forall d \in \mathcal{D} \\
& \dot{E}_{2,c,d} \leq b_{c,d} \dot{E}_{max,c} && \forall c \in \{c_1, c_2\} \forall d \in \mathcal{D} \\
& b_{c,d} \dot{E}_{min,c} \leq \dot{E}_{2,c} && \forall c \in \{c_1, c_2\} \forall d \in \mathcal{D} \\
& \dot{E}_{1,c_3,d} \leq \dot{E}_{max,c_3} && \forall d \in \mathcal{D} \\
& \dot{E}_{min,c} = 0.2 \dot{E}_{max,c} && \forall c \in \{c_1, c_2\} \\
& \dot{E}_{max,c_1} \leq 10 \\
& 60 \leq \dot{E}_{max,c_2}
\end{aligned}
$$

with

$$\mathbf{x} = [\dot{E}_{max,c_1}, \dot{E}_{max,c_2}, \dot{E}_{max,c_3}, \dot{E}_{min,c_1}, \dot{E}_{min,c_2}]$$
$$\mathcal{X} = \mathbb{R}^5_{\geq 0}$$
$$\mathbf{z} = [\dot{E}_{1,c_1,1}, \dots, \dot{E}_{1,c_1,|\mathcal{D}|}, \dot{E}_{1,c_2,1}, \dots, \dot{E}_{1,c_2,|\mathcal{D}|}, \dot{E}_{2,c_1,1}, \dots, \dot{E}_{2,c_1,|\mathcal{D}|}, \dot{E}_{1,c_3,1}, \dots, \dot{E}_{1,c_3,|\mathcal{D}|},$$
$$\dot{E}_{2,c_2,1}, \dots, \dot{E}_{2,c_2,|\mathcal{D}|}, b_{c_1,1}, \dots, b_{c_1,|\mathcal{D}|}, b_{c_2,1}, \dots, b_{c_2,|\mathcal{D}|}]$$
$$\mathcal{Z} = \mathbb{R}^{5|\mathcal{D}|}_{\geq 0} \times \{0,1\}^{2|\mathcal{D}|}$$

where $\dot{E}_{max,c}$ are the component capacities. For simplicity, a constant conversion efficiency of $\eta = 1$ between energy inflow $\dot{E}_1$ and energy outflow $\dot{E}_2$ is assumed. The operational constraints are enforced for every data point d in the historical data $\mathcal{D}$. Importantly, the allowed capacities for c_1 and c_2 differ and lead to a gap between the maximum output of component 1 and the minimal part-load of component 2.

Figure 6 illustrates the convex hull of the historical dataset and the feasible region of the design identified by the introduced problem. The infeasible region is approximated by sampling uniformly spaced energy demands and solving the corresponding operational feasibility problem. The worst-case scenario is identified by solving (MLP) using an adaptive discretization algorithm (Blankenship and Falk, 1976). Although all vertices of the convex hull are feasible, there are infeasible points inside the convex hull, introduced by the extra demand that is created when component c_2 has to be operated at minimal part-load.

2.4 Storage complementarity

Storage complementarity refers to the restriction that an energy storage device cannot simultaneously charge and discharge, which, according to Sass et al. (2020), can be expressed as

$$\dot{E}_{sto,in}\dot{E}_{sto,out} = 0,$$

where $\dot{E}_{sto,in}$ is the storage energy inflow and $\dot{E}_{sto,out}$ is the storage energy outflow. This nonconvex constraint is often applied when modeling battery systems (Appino et al., 2018; Sass et al., 2020). At the cell level, it is physically justified because the redox reaction proceeds in only one direction, depending on the applied potential (Goodenough and Kim, 2010). At the system level, simultaneous charging and discharging is also undesirable, as repeated cycling accelerates degradation (Kabir and Demirocak, 2017).

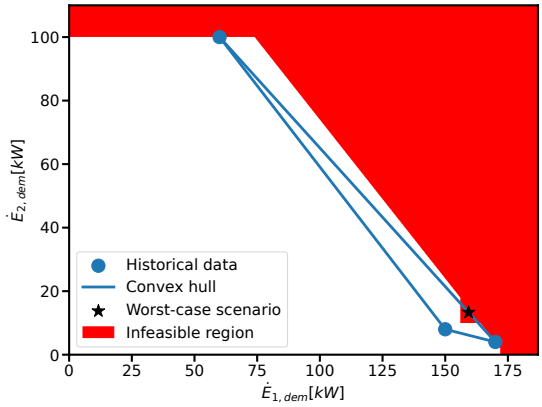

Fig. 6. Counter example for minimal part-load. The system schematic is shown in Figure 5. The figure illustrates how a design obtained using the feasibility time-step heuristic can be infeasible within the convex hull of the historical demand data. The convex hull of historical demand data for energy forms 1 and 2 is shown in blue, while the infeasible region is shaded in red. The worst-case scenario within the convex hull is marked by a star.

Simultaneous charging and discharging can be interpreted as a form of curtailment, since the associated losses lead to energy dissipation. In the following, we show that, if curtailment is allowed, storage complementarity does not affect the robustness of designs obtained using the feasibility time-step heuristic. We achieve this by demonstrating that if storage complementarity is neglected during operational optimization, a feasible schedule with the same objective function that satisfies complementarity can be recovered in a post-processing step by adjusting the storage operation while preserving the trajectory of the storage level. Since the operational problem is convex if storage complementarity is neglected, assuming no other nonconvexities are present, the design identified by the feasibility time-step heuristic is guaranteed to be robust. Automatically, this design is then also robust for the same operational problem with enforced complementarity, as we can then construct a feasible complementarity respecting schedule for every uncertainty realization.

In contrast, if curtailment is prohibited, this post-processing step is no longer applicable. Storage complementarity must then be enforced during optimization, introducing a nonconvexity that may result in non-robust designs.

We model the storage according to Sass et al. (2020). The following constraints have to be satisfied

by a feasible storage schedule:

$$0 \leq \dot{E}_{sto,out,t} \leq \dot{E}_{sto,out,max} \qquad \forall t \in \mathcal{T} \tag{3}$$

$$0 \leq \dot{E}_{sto,in,t} \leq \dot{E}_{sto,in,max} \qquad \forall t \in \mathcal{T} \tag{4}$$

$$E_{sto,t}\left(1 + \frac{\Delta_t}{\tau}\right) - E_{sto,t-1} = \Delta_t \left(\eta_{in}\dot{E}_{sto,in,t} - \frac{1}{\eta_{out}}\dot{E}_{sto,out,t}\right) \qquad \forall t \in \mathcal{T} \tag{5}$$

$$\dot{E}_{agg,t} + \dot{E}_{sto,in,t} - \dot{E}_{sto,out,t} \leq 0 \qquad \forall t \in \mathcal{T} \tag{6}$$

Here, $E_{sto,t}$ denotes the storage level, $\dot{E}_{sto,in,t}$ and $\dot{E}_{sto,out,t}$ are the energy inflows and outflows of the storage, t are the timesteps and $\mathcal{T}$ is the set of all timesteps, Δ_t is the timestep length, τ is the time constant for energy loss, and η_{in} and η_{out} are the charging and discharging efficiencies. The differential equation describing the storage of a generic storage is written as

$$\frac{\mathrm{d}E_{sto}}{\mathrm{d}t} = \eta_{in}\dot{E}_{sto,in} - \frac{1}{\eta_{out}}\dot{E}_{sto,out} - \frac{1}{\tau}E_{sto},$$

which we discretize using the implicit Euler scheme to obtain

$$E_{sto,t} = E_{sto,t-1} + \Delta_t \left(\eta_{in}\dot{E}_{sto,in,t} - \frac{1}{\eta_{out}}\dot{E}_{sto,out,t} - \frac{1}{\tau}E_{sto,t}\right)$$

and rearrange to obtain the equation describing the change of storage (5). The balance equation (6) ensures that the energy demand is met or exceeded. $\dot{E}_{agg,t}$ aggregates the energy demand and the energy inflows and outflows of all other components and is introduced for ease of exposition.

Given a schedule $\left(\hat{E}_{sto,t}, \hat{\dot{E}}_{sto,in,t}, \hat{\dot{E}}_{sto,out,t}\right)$ that does no respect complementarity, a complementarity-respecting schedule can be constructed by determining $\left(\hat{E}_{sto,t}, \tilde{\dot{E}}_{sto,in,t}, \tilde{\dot{E}}_{sto,out,t}\right)$ such that the storage levels $\hat{E}_{sto,t}$ remain unchanged as is shown in the following. Substituting into (5) yields the condition

$$\Delta_t \left(\eta_{in}\hat{\dot{E}}_{sto,in,t} - \frac{1}{\eta_{out}}\hat{\dot{E}}_{sto,out,t}\right) = \Delta_t \left(\eta_{in}\tilde{\dot{E}}_{sto,in,t} - \frac{1}{\eta_{out}}\tilde{\dot{E}}_{sto,out,t}\right) \tag{7}$$

Enforcing complementarity requires setting either $\tilde{\dot{E}}_{sto,in,t} = 0$ (discharging) or $\tilde{\dot{E}}_{sto,out,t} = 0$ (charging). Which variable is set to zero is determined by evaluating the right-hand side of Equation (5):

$$\eta_{in}\hat{\dot{E}}_{sto,in,t} - \frac{1}{\eta_{out}}\hat{\dot{E}}_{sto,out,t}$$

Solving Equation (7) for the remaining variable gives two cases:

$$(\tilde{\dot{E}}_{sto,in,t}, \tilde{\dot{E}}_{sto,out,t}) = \begin{cases} \left(0,\ \hat{\dot{E}}_{sto,out,t} - \eta_{in}\eta_{out}\hat{\dot{E}}_{sto,in,t}\right), & \text{if } \eta_{in}\hat{\dot{E}}_{sto,in,t} - \frac{1}{\eta_{out}}\hat{\dot{E}}_{sto,out,t} \leq 0, \\ \left(\hat{\dot{E}}_{sto,in,t} - \frac{1}{\eta_{in}\eta_{out}}\hat{\dot{E}}_{sto,out,t},\ 0\right), & \text{if } \eta_{in}\hat{\dot{E}}_{sto,in,t} - \frac{1}{\eta_{out}}\hat{\dot{E}}_{sto,out,t} > 0 \end{cases}$$

First, consider the case

$$\eta_{in}\hat{\dot{E}}_{sto,in,t} - \frac{1}{\eta_{out}}\hat{\dot{E}}_{sto,out,t} \leq 0$$

and

$$\tilde{\dot{E}}_{sto,out,t} = \hat{\dot{E}}_{sto,out,t} - \eta_{in}\eta_{out}\hat{\dot{E}}_{sto,in,t}$$

Feasibility is verified as follows. Since $\eta_{in}\eta_{out}\hat{\dot{E}}_{sto,in,t} \geq 0$,

$$\tilde{\dot{E}}_{sto,out,t} = \hat{\dot{E}}_{sto,out,t} - \underbrace{\eta_{in}\eta_{out}\hat{\dot{E}}_{sto,in,t}}_{\geq 0} \leq \hat{\dot{E}}_{sto,out,t} \leq \dot{E}_{sto,out,max}$$

Together with nonnegativity, i.e., $\tilde{\dot{E}}_{sto,out,t} = \left(\hat{\dot{E}}_{sto,out,t} - \eta_{in}\eta_{out}\hat{\dot{E}}_{sto,in,t}\right) \geq 0$, which follows from the case condition, Constraint (3) is satisfied. Trivially $\tilde{\dot{E}}_{sto,in,t} = 0$ satisfies Constraint (4). It remains to verify the balance constraint (6):

$$\dot{E}_{agg,t} - \tilde{\dot{E}}_{sto,out,t} = \dot{E}_{agg,t} - \left(\hat{\dot{E}}_{sto,out,t} - \eta_{in}\eta_{out}\hat{\dot{E}}_{sto,in,t}\right) \overset{!}{\leq} \dot{E}_{agg,t} - \left(\hat{\dot{E}}_{sto,out,t} - \hat{\dot{E}}_{sto,in,t}\right) \leq 0$$

To ensure $\dot{E}_{agg,t} - \left(\hat{\dot{E}}_{sto,out,t} - \eta_{in}\eta_{out}\hat{\dot{E}}_{sto,in,t}\right) \overset{!}{\leq} \dot{E}_{agg,t} - \left(\hat{\dot{E}}_{sto,out,t} - \hat{\dot{E}}_{sto,in,t}\right)$ it is sufficient that $\eta_{in}\eta_{out} \leq 1$. For physically consistent storage systems, the charging and discharging efficiencies fullfill $0 \leq \eta_{in} \leq 1$ and $0 \leq \eta_{out} \leq 1$ and hence $\eta_{in}\eta_{out} \leq 1$ holds. Otherwise, the storage would generate energy when charging or discharging. Therefore, the balance constraint (6) is satisfied.

Importantly, if curtailment is not allowed, the schedule needs to satisfy the balance constraint (6) with equality

$$\dot{E}_{agg,t} - \tilde{\dot{E}}_{sto,out,t} = \dot{E}_{agg,t} - \left(\hat{\dot{E}}_{sto,out,t} - \eta_{in}\eta_{out}\hat{\dot{E}}_{sto,in,t}\right) \overset{!}{=} \dot{E}_{agg,t} - \left(\hat{\dot{E}}_{sto,out,t} - \hat{\dot{E}}_{sto,in,t}\right) = 0,$$

which is only the case for $\eta_{in}\eta_{out} = 1$. Hence, for $\eta_{in} < 1$ or $\eta_{out} < 1$, complementarity must be enforced in the operational problem, which introduces a nonconvexity that may lead to designs identified by the feasibility time-step heuristic not being robust.

Now consider the case

$$\eta_{in}\hat{\dot{E}}_{sto,in,t} - \frac{1}{\eta_{out}}\hat{\dot{E}}_{sto,out,t} > 0$$

and

$$\tilde{\dot{E}}_{sto,in,t} = \hat{\dot{E}}_{sto,in,t} - \frac{1}{\eta_{in}\eta_{out}}\hat{\dot{E}}_{sto,out,t}$$

Feasibility follows similarly:

$$\tilde{\dot{E}}_{sto,in,t} = \hat{\dot{E}}_{sto,in,t} - \underbrace{\frac{1}{\eta_{in}\eta_{out}}\hat{\dot{E}}_{sto,out,t}}_{\geq 0} \leq \hat{\dot{E}}_{sto,in,t} \leq \dot{E}_{sto,in,max}$$

Together with nonnegativity, which follows from the case condition, Constraint (4) is satisfied. Trivially $\tilde{\dot{E}}_{sto,out,t} = 0$ satisfies Constraint (3). Again, the balance constraint has to hold:

$$\dot{E}_{agg,t} + \tilde{\dot{E}}_{sto,in,t} = \dot{E}_{agg,t} + \left(\hat{\dot{E}}_{sto,in,t} - \frac{1}{\eta_{in}\eta_{out}}\hat{\dot{E}}_{sto,out,t}\right) \overset{!}{\leq} \dot{E}_{agg,t} + \left(\hat{\dot{E}}_{sto,in,t} - \hat{\dot{E}}_{sto,out,t}\right) \leq 0,$$

which again holds true if $\eta_{in}\eta_{out} \leq 1$.

Summing up, as long as $\eta_{in}\eta_{out} \leq 1$, which is the physically relevant case, storage complementarity can be neglected if curtailment is allowed, as a feasible complementarity-respecting schedule can always be constructed in post-processing, guaranteeing that designs identified by the feasibility time-step heuristic are robust.

2.5 Guidelines and mitigating factors

Table 1 summarizes our results from this section and indicates the cases in which the feasibility time-step heuristic is guaranteed to identify robust designs.

	Curtailment	No-curtailment
Piecewise-linear convex energy inflow-outflow curve	✓	✗
Piecewise-linear nonconvex energy inflow-outflow curve	✗	✗
Minimal part-load	✗	✗
Storage complementarity	✓	✗
Objective function not jointly convex in $\mathbf{y}$ and $\mathbf{z}$	✗	✗

Tab. 1. Overview of common types of nonconvexities: A checkmark indicates that the feasibility time-step heuristic is guaranteed to yield a robust design despite the nonconvexity, whereas a cross indicates that the design may not be robust. Piecewise-linear energy inflow-outflow curves are separated by the convexity of the piecewise-linear curve, as piecewise-linear convex curves can be modeled fully linear if curtailment is allowed.

If the objective function of (MLP) is not jointly convex in the uncertainties and the operational

variables, the feasibility time-step method does not, in general, guarantee robust designs. In the absence of curtailment, any nonconvexity can lead to solutions that are not robust. In contrast, if curtailment is allowed, storage complementarity and piecewise-linear convex energy inflow-outflow curves do not compromise the robustness of designs identified by the heuristic. However, nonconvex energy inflow-outflow curves or minimal part-loads may lead the feasibility time-step heuristic to fail. We have shown small single-time-step examples for which the design identified by the feasibility time-step heuristic is infeasible within the convex hull of historical data.

If storage components are included in the design, coupling between time steps increases system flexibility by allowing energy to be shifted across timesteps. In the minimal part-load case, storage may compensate for low-demand periods where the installed components cannot operate at or below their minimal part-load by shifting generated energy flow from other timesteps. Similarly, energy losses in storage by simultaneous charging and discharging (e.g., thermal energy storage) can act as a weak form of curtailment. However, this curtailment is limited and hard to estimate a priori.

In general, the feasibility time-step heuristic can always be used to identify candidate designs. Nevertheless, when the problematic nonconvexities identified in Table 1 are present, verifying the feasibility of the design is recommended. At the current time, this can only be achieved by solving (MLP) to global optimality given the identified design, an approach that may quickly become computationally intractable.

3 Illustrative energy system example

We investigate an illustrative example based on the work by (Sass et al., 2020) and (Voll et al., 2013), which contains all of the previously discussed nonconvexities. We modify the case study from Sass et al. (2020) by removing the connection to the electricity grid, leading to an island multi-energy system; the only imported energy source is gas, used to power the CHPs and boilers. Figure 7 showcases the investigated system. Up to two copies of each component may be installed. For the CHPs, three categories are available: small, medium, and large, with different nominal capacity ranges and economic data. Unlike Sass et al. (2020), we only investigate the minimization of the total annualized cost (TAC) of the energy system and do not investigate the global warming impact, as our focus lies on investigating the robustness of the identified designs.

The data for the demands, solar irradiation, and ambient temperature is obtained from Sass et al. (2020) and accessible at Helmholtz Energy Computing Initiative (HECI) (2019). To construct representative days from the historical data, we follow the data preprocessing methodology of our previous work (Wedemeyer et al., 2026). The data is separated into days and resampled to 12 timesteps per day,

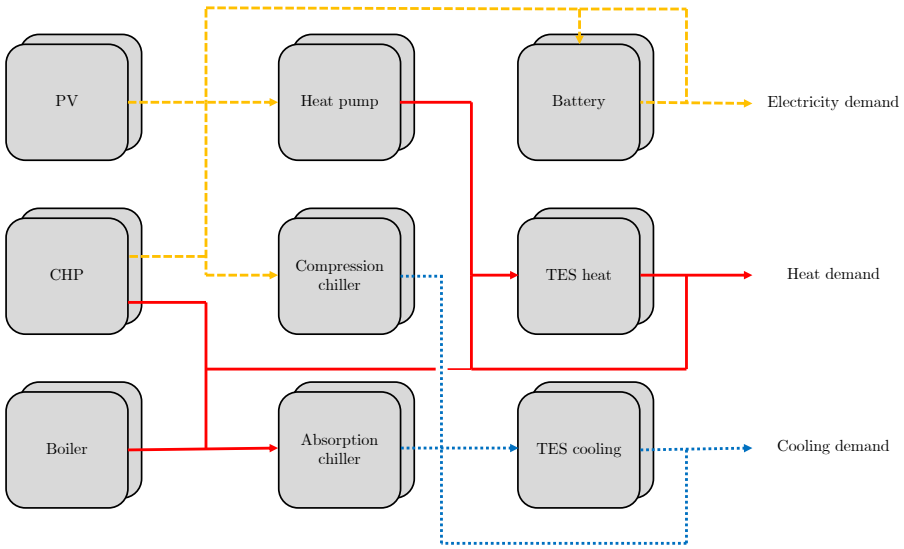

Fig. 7. Illustration of the modified example system based on Sass et al. (2020). Here, no connection to the electrical grid is present. Up to two copies of each component may be installed. For the CHPs, three categories are available: small, medium, and large, with different nominal capacity ranges and economic data. Note that the gas inflow into the CHP and boiler components is omitted from the illustration, as gas is externally supplied. Thermal energy storage units are abbreviated by TES.

then normalized to have unit variance and zero mean, and clustered into 4 representative scenarios using k-means clustering (MacQueen et al., 1967). All components are modeled according to Sass et al. (2020). The investigated system contains components with piecewise-linear performance curves. We noticed that the piecewise-linear performance curves provided by Sass et al. (2020) are nonconvex and do not fit with the provided original nonlinear curves. Furthermore, they also disagree with the piecewise linearizations provided by Voll et al. (2013) on which the work of Sass et al. (2020) is based. Hence, we re-linearized the nonlinear performance curves provided by Sass et al. (2020). For our linearization method and results, see Section 1 in the supplementary material. Additionally, the linearization data by Sass et al. (2020) suggests different minimal part-loads for the electricity and heat output of the CHPs. We follow the approach of Voll et al. (2013), who assume a shared minimal part-load of 0.5.

For a complete description of the used parameters and the optimization model, we refer to Section 2 of the supplementary material.

The linearized energy inflow-outflow curves of the boiler, CHP, and heat pump only have a single linear segment and are hence convex. The PV system and the energy storages are modeled with constant efficiencies. Only the linearized energy inflow-outflow curves of compression and absorption chillers are modeled with two linear segments each, and the curves are convex too. The battery is modeled with

charging complementarity constraints. However, those can be neglected with respect to robustness as described in Section 2.4. Regarding joint convexity of the objective function, the nominal efficiency of the heat pump depends on the uncertain ambient temperature and enters the lower-level problem as follows:

$$\dot{E}_{e_{in},hp,t} - \frac{\dot{E}_{e_{out},hp,t}}{\eta_{hp,nom,t}(T_{amb,t})} = 0$$

To remove the coupling equality constraint, we directly insert this definition of the energy inflow into the energy balance, cf. Section 2.1. The resulting term is not jointly convex in $\mathbf{y}$ and $\mathbf{z}$ and hence may lead to a failure of the feasibility timestep heuristic (Teichgraeber et al., 2020).

Consequently, from the preceding analysis, the only sources of nonconvexity in this case study that may cause the feasibility time-step heuristic to fail are the objective function not being jointly convex and the presence of minimal part-load constraints. We determine a candidate robust design using the feasibility time-step heuristic (Teichgraeber et al., 2020) and investigate its robustness.

3.1 Rigorously verifying robustness

To validate the robustness of the candidate design generated by the feasibility time-step heuristic (Teichgraeber et al., 2020) and to determine whether minimal part-load constraints or joint nonconvexities in the objective function introduce infeasibilities, we solve problem (MLP) to rigorously identify the maximum violation within the convex hull of the historical data.

(MLP) is a challenging bilevel problem, and preliminary numerical experiments showed prohibitively long convergence times when using adaptive-discretization approaches (Blankenship and Falk, 1976). Furthermore, the presence of integer variables renders the lower-level problem nonconvex, making common single-level reformulation approaches based on the KKT-optimality conditions (Fortuny-Amat and McCarl, 1981) or the linear dual (Burgard et al., 2003) inapplicable. To address this issue, we propose a hybrid approach that combines elements of classical adaptive discretization methods (Blankenship and Falk, 1976) with a single-level reformulation by embedding the linear dual of the lower-level problem (Burgard et al., 2003). Specifically, we apply an adaptive discretization approach to the integer variables and then embed the dual of the resulting linear program into the medial-level problem for each set of discretized integer variables.

Our approach is similar to that proposed in Mitsos (2010), where the KKT conditions are used to tighten the lower bounding scheme to solve a mixed-integer bilevel program. In contrast, we do not introduce a parametric upper bound on the objective value of the lower-level problem and instead embed

the linear dual at each discretization point.

$$\min_{\mathbf{z}_c \in \mathbb{R}^{n_c}, \mathbf{z}_d \in \{0,1\}^{n_d}} \quad \mathbf{c}_c^T \mathbf{z}_c \tag{LLP}$$
$$\text{s.t.} \quad \mathbf{A}_c(\mathbf{y})\mathbf{z}_c \leq \mathbf{b}(\mathbf{y}) - \mathbf{A}_d \mathbf{z}_d$$

To this end, we first introduce how we form the dual of the lower-level problem with fixed integer variables that is then embedded into the medial-level problem. (LLP) shows the lower-level problem, rewritten in inequality-constrained form without explicit bounds on the continuous variables, which have been moved to the constraints, to simplify the dual formulation. For a general treatment of dual problems of linear programs, see Bertsimas and Tsitsiklis (1997). Here, $\mathbf{c}_c$ is the cost vector and $\mathbf{A}_c(\mathbf{y})$ and $\mathbf{A}_d$ are the coefficient matrices for the linear constraints for the continuous and integer variables, respectively. $\mathbf{A}_c(\mathbf{y})$ may be a function of the medial-level variables. For example in the present case study, the uncertain variables include ambient temperatures $T_{amb,t}$, which affect the efficiency of the heat pumps: $\eta_{hp,nom,t}(T_{amb,t}) = \frac{0.36 T_{hp}}{T_{hp} - T_{amb,t}}$, where T_{hp} is the output temperature of the heat pump (Sass et al., 2020) and may appear in the lower-level program in constraints as $\dot{E}_{e_{in},hp,t} - \frac{\dot{E}_{e_{out},hp,t}}{\eta_{hp,nom,t}} = 0$. The vector $\mathbf{b}(\mathbf{y})$ denotes the right-hand side of the constraints and depends linearly on the medial-level variables $\mathbf{y}$.

Importantly, we assume here that (LLP) corresponds to the lower level of an SIP or has been transformed into an SIP by moving the coupling constraints into the objective function, as described in Section 2. Under this assumption, the dependence of $\mathbf{A}_c(\mathbf{y})$ and $\mathbf{b}(\mathbf{y})$ on the medial-level variables $\mathbf{y}$ results solely from the reformulation of the nonlinear maximum terms in the objective function of the medial-level problem (1) into an equivalent linear form (cf., Chapter 1.3 in Bertsimas and Tsitsiklis (1997) and Section 3.2.2 in Varelmann et al. (2022)).

When forming the dual, the integer variables $\mathbf{z}_d$ are fixed and therefore appear as constants on the right-hand side. Forming the dual of problem (LLP) with fixed integer variables $\bar{\mathbf{z}}_d$ yields problem (LLP dual).

$$\max_{\boldsymbol{\lambda} \in \mathbb{R}^{n_{cs}}_{\leq 0}} \quad \boldsymbol{\lambda}^T \left(\mathbf{b}(\mathbf{y}) - \mathbf{A}_d \bar{\mathbf{z}}_d\right) \tag{LLP dual}$$
$$\text{s.t.} \quad \boldsymbol{\lambda}^T \mathbf{A}_c(\mathbf{y}) = \mathbf{c}_c^T$$

In contrast to classical adaptive discretization methods, which discretize all lower-level variables (Blankenship and Falk, 1976; Djelassi and Mitsos, 2021), we discretize only the integer variables $\mathbf{z}_d$. Let $\bar{\mathbf{z}}_{d,k}$ denote a fixed realization of the integer variables corresponding to discretization index $k \in \mathcal{K}$.

The resulting discretized medial-level problem can be written as

$$\max_{\mathbf{y}\in\mathcal{Y},\phi\in\mathbb{R}} \quad \phi \tag{MLP-disc}$$
$$\text{s.t.} \quad \phi \leq \min_{\mathbf{z}_{c,k}\in\mathcal{Z}_{disc}(\mathbf{y},\bar{\mathbf{z}}_{d,k})} \quad \mathbf{c}_c^T\mathbf{z}_{c,k} \;\; \forall k \in \mathcal{K}$$

Here, ϕ is an auxiliary variable that ensures that the objective is smaller than the optimal value of any of the discretizations so far, and $\mathcal{Z}_{disc}(\mathbf{y},\bar{\mathbf{z}}_{d,k}) = \{\mathbf{z}_c \mid \mathbf{A}_c(\mathbf{y})\mathbf{z}_c \leq \mathbf{b}(\mathbf{y}) - \mathbf{A}_d\bar{\mathbf{z}}_{d,k}), \mathbf{z}_c \in \mathbb{R}^{n_c})\}$ denotes the feasible set for the continuous lower-level variables.

Since the objective here is to verify the robustness of a given design, the design variables $\mathbf{x}$ are treated as fixed and their dependence is omitted from the notation for simplicity, unlike in problem (MLP).

(MLP-disc) is a bi-level problem. To obtain a single-level formulation, we replace the embedded lower-level problem by its dual for each discretization point:

$$\max_{\mathbf{y}\in\mathcal{Y},\phi\in\mathbb{R},\boldsymbol{\lambda}_k\in\mathbb{R}^{n_{cs}}_{\leq 0}\forall k\in\mathcal{K},\mathbf{z}_{c,k}\in\mathbb{R}^{n_c}\forall k\in\mathcal{K}} \quad \phi \tag{MLP-dual-disc}$$
$$\begin{aligned}
\text{s.t.} \quad & \phi \leq \boldsymbol{\lambda}_k^T\left(\mathbf{b}(\mathbf{y}) - \mathbf{A}_d\bar{\mathbf{z}}_{d,k}\right) && \forall k \in \mathcal{K}\\
& \boldsymbol{\lambda}_k^T\mathbf{A}_c(\mathbf{y}) = \mathbf{c}_c^T && \forall k \in \mathcal{K}\\
& \mathbf{A}_c(\mathbf{y})\mathbf{z}_{c,k} \leq \mathbf{b}(\mathbf{y}) - \mathbf{A}_d\bar{\mathbf{z}}_{d,k} && \forall k \in \mathcal{K}\\
& \boldsymbol{\lambda}_k^T\left(\mathbf{b}(\mathbf{y}) - \mathbf{A}_d\bar{\mathbf{z}}_{d,k}\right) = \mathbf{c}_c^T\mathbf{z}_{c,k} && \forall k \in \mathcal{K}
\end{aligned}$$

Note that we additionally embed the primal constraints and set the primal and dual objective equal, as we found this to improve performance in preliminary studies.

(MLP) is then solved iteratively, similar to the algorithm of Blankenship and Falk (1976): In each iteration, a worst-case candidate $\mathbf{y}$ is determined by solving problem (MLP-dual-disc). The lower-level problem (LLP) is subsequently solved to obtain a new realization of the integer variables, which is added to the discretization set. The discretization set is initialized with the integer variable values of the solution to the operational problem for the historical data point with the highest objective value. This procedure is repeated until convergence.

In each iteration of the adaptive discretization algorithm, the dual formulation corresponding to an additional integer discretization point is added to problem (MLP-dual-disc). Furthermore, the terms $\boldsymbol{\lambda}_k^T\mathbf{b}(\mathbf{y})$ and $\boldsymbol{\lambda}_k^T\mathbf{A}_c(\mathbf{y})$ lead to bilinear constraints with respect to the medial-level variables $\mathbf{y}$ and the dual variables $\boldsymbol{\lambda}_k$. As a result, the optimization problem grows rapidly and becomes computationally challenging. Consequently, the size of the problem that can be solved is limited, and we restrict the

Component	Initial SOC as 50% of nominal capacity	Variable initial SOC
Boiler	441 kW	433 kW
CHP	328 kW	331 kW
Heat pump	153 kW	150 kW
Compression Chiller	400 kW	400 kW
TES cooling	1735 kW h	1636 kW h

Tab. 2. Nominal capacitities of the installed components for the case where the initial state of charge (SOC) of the storages is fixed to half of the nominal capacity (Nominal capacity) and for the case where the initial SOC is a design variable.

number of timesteps per day in order to maintain tractability.

3.2 Robustness of the identified design

We verify the robustness of the candidate design for the illustrative case study using the method presented in the previous subsection. Despite the removal of the electrical grid connection and modified parameters for the piecewise-linear input–output relations, the resulting system design is similar to the low total annualized cost design reported in the original publication by Sass et al. (2020). The installed conversion components are a boiler, a small CHP plant, a heat pump, and a compression chiller. The only installed storage component is a thermal energy storage (TES) unit for cooling.

Compared to the low-TAC design in Sass et al. (2020), the design identified in our study includes a heat pump but no heat storage. This difference is likely due to the removal of the electrical grid connection. Excess electricity produced by the CHP can no longer be exported to the grid and is instead converted into heat using the heat pump. The installed capacities are given in Table 2.

Version 13.0.0 of the Gurobi optimizer (Gurobi Optimization, LLC, 2025) is used to solve all subproblems. For the design problem in the feasibility time-step heuristic, we set the 'MIPGap' parameter to 0.005, i.e., a relative optimality gap of 0.5%, as solving the design problem to global optimality took prohibitively long, likely due to the large number of integer variables. Other than that, the default parameters were used. In total, seven iterations of the adaptive discretization algorithm (Section 3.1) were required, i.e., seven realizations of the binary on–off variables were sufficient to cover all relevant uncertainty realizations. This comparatively small number of discretization points is notable. With four installed components and twelve timesteps, the number of possible on–off combinations is 4^{12}. The limited number of active discretization points is likely due to two factors. First, the boiler and CHP are externally supplied components and can therefore always be operated at maximum capacity, as their input energy is externally supplied. Second, the installed cooling storage allows demand to be shifted between timesteps, which reduces the number of distinct operational patterns required to cover the uncertainty

realizations.

Importantly, solving (MLP) identifies a scenario within the convex hull of the historical data for which a violation of 1.1 kW occurs, i.e., the design is not robust. The violation is small and occurs in the electricity balance; the demand at the corresponding time step is 313.6 kW. To model the energy storage, we assume a cyclical constraint, i.e., the last time step of each scenario is connected to the first. Furthermore, we assume that in the first time step, the initial state of charge (SOC) is at 50%. This introduces an additional cooling demand even on days where no cooling is required, as the energy dissipated by the TES needs to be compensated. Hence, a second run is performed where the initial storage level is a design variable in the upper-level. The resulting capacities for the variable initial SOC case are shown in the right column of Table 2. Overall, the design is very similar to the design without a variable initial state of charge, with slight deviations in capacity for most components. The initial SOC of the TES for cooling is 278 kW h, which corresponds to 17% and is less than in the fixed SOC case. No infeasible scenarios were identified within the convex hull of the historical data by solving (MLP) for this design, hence it is robust.

4 Conclusion

Identifying energy system designs that can meet demand under any uncertainty realization in the predefined uncertainty set is crucial to ensure reliable energy supply. To this end, heuristic approaches such as the feasibility time-step heuristic (Teichgraeber et al., 2020) have been applied, e.g., Bahl et al. (2017b). This is because rigorous solution approaches, such as our robust energy system design approach (Wedemeyer et al., 2026), quickly become computationally intractable as system size and temporal resolution increase. However, if the operational problem contains nonconvexities, the robustness of designs identified by this heuristic is not guaranteed.

This study provides a critical theoretical and empirical validation of the feasibility time-step heuristic in the context of nonconvex MILP energy system models. We identify 3 common nonconvexities in MILP energy system models that affect robustness: piecewise-linear modeling of energy inflow-outflow behavior, minimal part loads, and storage complementarity constraints. Additionally, care must be taken to identify how the uncertain variables $\mathbf{y}$ enter the lower-level problem. If the objective function of the lower-level problem is not convex in $\mathbf{y}$, the feasibility timestep heuristic may fail even if the lower-level problem is convex in $\mathbf{z}$.

Our analysis shows that if curtailment of surplus energy flows is not allowed, any of these nonconvexities may lead to infeasible designs when using the feasibility time-step heuristic (Teichgraeber

et al., 2020). If curtailment is permitted, however, most of these issues disappear. In particular, convex piecewise-linear input–output relations constitute only an apparent nonconvexity and can be reformulated as linear constraints, while storage complementarity can be ignored. Under these conditions, minimal part-load constraints remain the primary source of potential infeasibility, although storage can partially mitigate their impact by shifting energy between timesteps.

To rigorously verify robustness, we propose a hybrid approach that combines adaptive discretization (Blankenship and Falk, 1976) with duality-based single-level reformulations (Fortuny-Amat and McCarl, 1981; Burgard et al., 2003) to verify the robustness of designs identified by the feasibility time-step heuristic. While this approach provides a formal verification procedure, it leads to a quadratically constrained optimization problem whose size grows with each discretization iteration and is therefore computationally demanding.

We apply the hybrid approach to an illustrative case study based on Sass et al. (2020) and Voll et al. (2013). A candidate design is first identified using the feasibility time-step heuristic (Teichgraeber et al., 2020) and subsequently verified using the hybrid method. A scenario within the convex hull of the historical data is identified, for which a small infeasibility of 1.1 kW arises. The mismatch occurs in the electricity balance, and the demand at the timestep where the violation occurs is 313.6 kW. We resolve the problem by allowing the initial state of charge of storage components to be determined by the optimizer. Despite the presence of minimal part-load constraints and the objective function being nonconvex in the nominal efficiency of the heat pump, which is uncertain due to its dependence on ambient temperature, the identified design is shown to be robust for all uncertainty realizations within the convex hull of the historical data. Together with the theoretical analysis of the relevant nonconvexities, this result demonstrates that the feasibility time-step heuristic can yield robust designs even when the operational problem is formulated as an MILP problem and nonconvexity in the uncertain variables is present. However, the fact that the design with a fixed initial state of charge was proven not to be robust highlights that care must be taken when applying the feasibility timestep heuristic.

Interestingly, we were unable to identify any conversion components with inherently nonconvex input–output energy flow relations. Future work may investigate whether there is a thermodynamic basis substantiating this observation. Moreover, the development of computationally efficient methods for verifying the robustness of candidate designs remains an important direction for future research, as the proposed hybrid method quickly becomes computationally infeasible for large-scale problems.

Acknowledgment

This work was performed as part of the Helmholtz School for Data Science in Life, Earth and Energy (HDS-LEE) and received funding from the Helmholtz Association of German Research Centres. We further acknowledge financial support by the Helmholtz Association of German Research Centres through program-oriented funding. Special thanks to Susanne Sass and Dinah Elena Hollermann for clarifying the mapping of the linearization parameters.

Data availability

Data will be made available on request.

Declaration of competing interests

The authors declare that they have no known competing financial interests or personal relationships that could have appeared to influence the work reported in this paper.

Authors' contributions

Conceptualization: M.W., A.M., M.D.; Methodology: M.W.; Software: M.W.; Formal analysis and investigation: M.W.; Visualization: M.W.; Writing - original draft preparation: M.W.; Writing - review and editing: A.M., M.D.; Funding acquisition: A.M., M.D.; Supervision: A.M., M.D.

Declaration of generative AI and AI-assisted technologies in the manuscript preparation process.

During the preparation of this work, M.W. used ChatGPT in order to correct grammar and spelling and to improve the style of writing. After using this tool, all authors reviewed and edited the content as needed and take full responsibility for the content of the publication.

Nomenclature

Abbreviations

ESIP	Existence-constrained semi-infinite program
GSIP	Generalized semi-infinite program
MILP	Mixed-integer linear programming
SOC	State of charge
TAC	Total annualized cost
TES	Thermal energy storage

Greek symbols

β	Slope parameter
Δ_t	Timestep length
η	Efficiency
λ	Linearization parameter
$\boldsymbol{\lambda}$	Dual variables
τ	Time constant for energy loss
ϕ	Auxillary variable

Latin symbols

$\mathbf{A}_c(\mathbf{y})$	Constraint matrix for continuous variables
$\mathbf{A}_d$	Constraint matrix for integer variables
b	Binary variable
$\mathbf{b}(\mathbf{y})$	Right hand side vector
c	Component
C	Set of components
$\mathbf{c}_c$	Cost vector
c_{inv}	Investment costs
c_{op}	Operational costs
d	Data point
$\mathcal{D}$	Historical data
e	Energy form
E	Energy
$\mathcal{E}$	Set of energy forms
$\dot{E}$	Energy flow
g	Constraint
$g_{en}(\mathbf{x}, \cdot, \cdot)$	Constraints for energy system model
$g_x(\mathbf{x})$	Design constraints
$g_y(\mathbf{x})$	Uncertainty bounds
$\mathcal{J}$	Index set
k	Discretization index
$\mathcal{K}$	Set of discretization indices
n_c	Dimensionality of continuous operational variables

n_{cs}	Number of constraints
n_d	Dimensionality of integer operational variables
n_x	Dimensionality of design variables
n_y	Dimensionality of uncertainty realizations
n_z	Dimensionality of operational variables
s	Scenario
$\mathcal{S}$	Set of scenarios
t	Time step
$\mathcal{T}$	Set of time steps
T_{amb}	Ambient temperature
$\mathbf{x}$	Design variables
$\mathcal{X}$	Feasible set of design variables
$\mathbf{y}$	Uncertainty realizations
$\mathcal{Y}$	Feasible set of uncertainty realizations
$\mathbf{z}$	Operational variables
$\mathbf{z}_c$	Continuous operational variables
$\mathbf{z}_d$	Integer operational variables
$\mathcal{Z}$	Feasible set of operational variables
$\mathcal{Z}_{disc}$	Feasible set of operational variables for fixed integer variables

Subscripts

agg	Aggregated
dem	Demand
in	Inflow
hp	Heat pump
j	Index
k	Discretization index
max	Maximum
min	Minimum
nom	Nominal

out	Outflow
s	Representative scenario
sto	Storage
t	Time step

References

Abdin, A.F., Caunhye, A., Zio, E., Cardin, M.A., 2022. Optimizing generation expansion planning with operational uncertainty: A multistage adaptive robust approach. Applied Energy 306, 118032. doi:10.1016/j.apenergy.2021.118032.

Appino, R.R., González Ordiano, J.Á., Mikut, R., Faulwasser, T., Hagenmeyer, V., 2018. On the use of probabilistic forecasts in scheduling of renewable energy sources coupled to storages. Applied Energy 210, 1207–1218. doi:10.1016/j.apenergy.2017.08.133.

Bahl, B., Kümpel, A., Seele, H., Lampe, M., Bardow, A., 2017a. Time-series aggregation for synthesis problems by bounding error in the objective function. Energy 135, 900–912. doi:10.1016/j.energy.2017.06.082.

Bahl, B., Lützow, J., Majewski, D.E., Lampe, M., Hennen, M., Bardow, A., 2017b. Rigorous synthesis of energy supply systems by time-series aggregation, in: Espuña, A., Graells, M., Puigjaner, L. (Eds.), Computer Aided Chemical Engineering. Elsevier. volume 40 of *27 European Symposium on Computer Aided Process Engineering*, pp. 2413–2418. doi:10.1016/B978-0-444-63965-3.50404-9.

Bahl, B., Lützow, J., Shu, D., Hollermann, D.E., Lampe, M., Hennen, M., Bardow, A., 2018. Rigorous synthesis of energy systems by decomposition via time-series aggregation. Computers & chemical engineering 112, 70 – 81. doi:10.1016/j.compchemeng.2018.01.023.

Baumgärtner, N., Bahl, B., Hennen, M., Bardow, A., 2019a. RiSES3: Rigorous Synthesis of Energy Supply and Storage Systems via time-series relaxation and aggregation. Computers & Chemical Engineering 127, 127–139. doi:10.1016/j.compchemeng.2019.02.006.

Baumgärtner, N., Temme, F., Bahl, B., 2019b. Rises4: Rigorous synthesis of energy supply systems with seasonal storage by relaxation and time-series aggregation to typical periods, in: Proceedings of the International Conference on Efficiency, Cost, Optimization, Simulation and Environmental Impact of Energy Systems (ECOS 2019), Institute of Thermal Technology. pp. 263–274.

Ben-Tal, A., El Ghaoui, L., Nemirovski, A.S., 2009. Robust Optimization. Princeton Series in Applied Mathematics, Princeton University Press, Princeton.

Ben-Tal, A., Goryashko, A., Guslitzer, E., Nemirovski, A., 2004. Adjustable robust solutions of uncertain linear programs. Mathematical Programming 99, 351–376. doi:10.1007/s10107-003-0454-y.

Bertsimas, D., Tsitsiklis, J.N., 1997. Introduction to Linear Optimization. Athena Scientific Series in Optimization and Neural Computation, Athena Scientific, Belmont, Mass.

Blankenship, J.W., Falk, J.E., 1976. Infinitely constrained optimization problems. Journal of Optimization Theory and Applications 19, 261–281. doi:10.1007/BF00934096.

Burgard, A.P., Pharkya, P., Maranas, C.D., 2003. Optknock: A bilevel programming framework for identifying gene knockout strategies for microbial strain optimization. Biotechnology and Bioengineering 84, 647–657. doi:10.1002/bit.10803.

Charnes, A., Cooper, W.W., Kortanek, K., 1962. Duality, haar programs, and finite sequence spaces. Proceedings of the National Academy of Sciences 48, 783–786. doi:10.1073/pnas.48.5.783.

Djelassi, H., 2020. Diskretisierungsbasierte Algorithmen für die globale Lösung hierarchischer Optimierungsprobleme. Dissertation, RWTH Aachen University. doi:10.18154/RWTH-2020-09163.

Djelassi, H., Glass, M., Mitsos, A., 2019. Discretization-based algorithms for generalized semi-infinite and bilevel programs with coupling equality constraints. Journal of Global Optimization 75, 341–392. doi:10.1007/s10898-019-00764-3.

Djelassi, H., Mitsos, A., 2021. Global Solution of Semi-infinite Programs with Existence Constraints. Journal of Optimization Theory and Applications 188, 863–881. doi:10.1007/s10957-021-01813-2.

Domínguez-Muñoz, F., Cejudo-López, J.M., Carrillo-Andrés, A., Gallardo-Salazar, M., 2011. Selection of typical demand days for CHP optimization. Energy and Buildings 43, 3036–3043. doi:10.1016/j.enbuild.2011.07.024.

Fleschutz, M., Bohlayer, M., Braun, M., Murphy, M.D., 2025. The hidden cost of using time series aggregation for modeling low-carbon industrial energy systems: An investors' perspective. Energy 318, 134615. doi:10.1016/j.energy.2025.134615.

Fortuny-Amat, J., McCarl, B., 1981. A Representation and Economic Interpretation of a Two-Level Programming Problem. Journal of the Operational Research Society 32, 783–792. doi:10.1057/jors.1981.156.

Gabrielli, P., Fürer, F., Mavromatidis, G., Mazzotti, M., 2019. Robust and optimal design of multi-energy systems with seasonal storage through uncertainty analysis. Applied Energy 238, 1192–1210. doi:10.1016/j.apenergy.2019.01.064.

Glover, F., 1975. Improved linear integer programming formulations of nonlinear integer problems. Management Science 22, 455–460. doi:10.1287/mnsc.22.4.455.

Goodenough, J.B., Kim, Y., 2010. Challenges for Rechargeable Li Batteries. Chemistry of Materials 22, 587–603. doi:10.1021/cm901452z.

Grossmann, I.E., Sargent, R.W.H., 1978. Optimum design of chemical plants with uncertain parameters. AIChE Journal 24, 1021–1028. doi:10.1002/aic.690240612.

Gurobi Optimization, LLC, 2025. Gurobi optimizer reference manual. https://www.gurobi.com (accessed 29 March 2026).

Halemane, K.P., Grossmann, I.E., 1983. Optimal process design under uncertainty. AIChE Journal 29, 425–433. doi:10.1002/aic.690290312.

Helmholtz Energy Computing Initiative (HECI), 2019. Heci energy benchmark repository. https://jugit.fz-juelich.de/heci/energy-benchmark (accessed 20 February 2026).

Hoffmann, M., Schyska, B.U., Bartels, J., Pelser, T., Behrens, J., Wetzel, M., Gils, H.C., Tang, C.F., Tillmanns, M., Stock, J., Xhonneux, A., Kotzur, L., Praktiknjo, A., Vogt, T., Jochem, P., Linßen, J., Weinand, J.M., Stolten, D., 2024. A review of mixed-integer linear formulations for framework-based energy system models. Advances in Applied Energy 16, 100190. doi:10.1016/j.adapen.2024.100190.

Kabir, M.M., Demirocak, D.E., 2017. Degradation mechanisms in Li-ion batteries: A state-of-the-art review. International Journal of Energy Research 41, 1963–1986. doi:10.1002/er.3762.

Kotzur, L., Markewitz, P., Robinius, M., Stolten, D., 2018. Impact of different time series aggregation methods on optimal energy system design. Renewable Energy 117, 474–487. doi:10.1016/j.renene.2017.10.017.

Kotzur, L., Nolting, L., Hoffmann, M., Groß, T., Smolenko, A., Priesmann, J., Büsing, H., Beer, R., Kullmann, F., Singh, B., Praktiknjo, A., Stolten, D., Robinius, M., 2021. A modeler's guide to handle complexity in energy systems optimization. Advances in Applied Energy 4, 100063. doi:10.1016/j.adapen.2021.100063.

MacQueen, J., et al., 1967. Some methods for classification and analysis of multivariate observations, in: Proceedings of the fifth Berkeley symposium on mathematical statistics and probability, Oakland, CA, USA. pp. 281–297.

Majewski, D.E., Lampe, M., Voll, P., Bardow, A., 2017. TRusT: A Two-stage Robustness Trade-off approach for the design of decentralized energy supply systems. Energy 118, 590–599. doi:10.1016/j.energy.2016.10.065.

Mancò, G., Tesio, U., Guelpa, E., Verda, V., 2024. A review on multi energy systems modelling and optimization. Applied Thermal Engineering 236, 121871. doi:10.1016/j.applthermaleng.2023.121871.

Mitsos, A., 2010. Global solution of nonlinear mixed-integer bilevel programs. Journal of Global Optimization 47, 557–582. doi:10.1007/s10898-009-9479-y.

Ommen, T., Markussen, W.B., Elmegaard, B., 2014. Comparison of linear, mixed integer and non-linear programming methods in energy system dispatch modelling. Energy 74, 109–118. doi:10.1016/j.energy.2014.04.023.

Sass, S., Faulwasser, T., Hollermann, D.E., Kappatou, C.D., Sauer, D., Schütz, T., Shu, D.Y., Bardow, A., Gröll, L., Hagenmeyer, V., Müller, D., Mitsos, A., 2020. Model compendium, data, and optimization benchmarks for sector-coupled energy systems. Computers & Chemical Engineering 135, 106760. doi:10.1016/j.compchemeng.2020.106760.

Shen, F., Zhao, L., Du, W., Zhong, W., Qian, F., 2020. Large-scale industrial energy systems optimization under uncertainty: A data-driven robust optimization approach. Applied Energy 259, 114199. doi:10.1016/j.apenergy.2019.114199.

Soyster, A.L., 1973. Technical Note—Convex Programming with Set-Inclusive Constraints and Applications to Inexact Linear Programming. Operations Research 21, 1154–1157. doi:10.1287/opre.21.5.1154.

Stein, O., 2003. Bi-Level Strategies in Semi-infinite Programming. volume 71 of *Nonconvex Optimization and Its Applications*. Softcover repr. of the hardcover 1. ed. ed., Springer Science+Business Media, New York, NY. doi:10.1007/978-1-4419-9164-5.

Stuber, M.D., Barton, P.I., 2015. Semi-Infinite Optimization with Implicit Functions. Industrial & Engineering Chemistry Research 54, 307–317. doi:10.1021/ie5029123.

Teichgraeber, H., Brandt, A.R., 2019. Clustering methods to find representative periods for the optimization of energy systems: An initial framework and comparison. Applied Energy 239, 1283–1293. doi:10.1016/j.apenergy.2019.02.012.

Teichgraeber, H., Lindenmeyer, C.P., Baumgärtner, N., Kotzur, L., Stolten, D., Robinius, M., Bardow, A., Brandt, A.R., 2020. Extreme events in time series aggregation: A case study for optimal residential energy supply systems. Applied Energy 275, 115223. doi:10.1016/j.apenergy.2020.115223.

Varelmann, T., Erwes, N., Schäfer, P., Mitsos, A., 2022. Simultaneously optimizing bidding strategy in pay-as-bid-markets and production scheduling. Computers & Chemical Engineering 157, 107610. doi:10.1016/j.compchemeng.2021.107610.

Voll, P., 2014. Automated optimization-based synthesis of distributed energy supply systems. Dissertation. RWTH Aachen University. Aachen. URL: https://publications.rwth-aachen.de/record/228954.

Voll, P., Klaffke, C., Hennen, M., Bardow, A., 2013. Automated superstructure-based synthesis and optimization of distributed energy supply systems. Energy 50, 374–388. doi:10.1016/j.energy.2012.10.045.

Wang, Y., Volkmer, M., Hagedorn, D.F., Reinert, C., von der Assen, N., 2024. RiNSES4: Rigorous Nonlinear Synthesis of Energy Systems for Seasonal Energy Supply and Storage. Systems and Control Transactions 3, 604–611. doi:10.69997/sct.105466.

Wedemeyer, M., Cramer, E., Mitsos, A., Dahmen, M., 2026. Robust energy system design via semi-infinite programming. Optimization and Engineering 27, 503–530. doi:10.1007/s11081-025-10016-x.

Wirtz, M., Hahn, M., Schreiber, T., Müller, D., 2021. Design optimization of multi-energy systems using mixed-integer linear programming: Which model complexity and level of detail is sufficient? Energy Conversion and Management 240, 114249. doi:10.1016/j.enconman.2021.114249.

Robust Design of Multi-Energy Systems Accounting for Mixed-Integer Operational Problems - Supplementary Material

Moritz Wedemeyer[a,b], Alexander Mitsos[d,a,c], Manuel Dahmen[a,*]

[a] Institute of Climate and Energy Systems, Energy Systems Engineering (ICE-1), Forschungszentrum Jülich GmbH, Jülich 52425, Germany

[b] RWTH Aachen University, Aachen 52062, Germany

[c] RWTH Aachen University, Process Systems Engineering (AVT.SVT), Aachen 52074, Germany

[d] JARA-ENERGY, Jülich 52425, Germany

1 Linearization

As mentioned in the main manuscript, we relinearize the energy inflow-outflow for all conversion components, i.e., boiler, CHP, absorption chiller (AC), compression chiller (CC), and the heat pump (HP), in the case study by Sass et al. (2020). To ensure that the piecewise energy inflow-outflow relationship closely approximates the original nonlinear relationship, we apply the following linearization procedure: We sample the nonlinear function at 250 equidistant points between the minimum part-load and the maximum part-load. We then minimize the sum of the squared residuals between a piecewise-linear function and the sampled points. The locations of the breakpoints of the piecewise-linear function are optimization variables, and we fix the output part-load of the lowest and highest breakpoints to be at the minimum and maximum part-load, respectively. To ensure comparability, we use the same number of breakpoints as Sass et al. (2020). Table 1 shows the parameters of the linearization, i.e., the relative input λ_{in}, which is the energy inflow $\dot{E}_{in}$ divided by the nominal capacity $\dot{E}_{nom}$ multiplied by the nominal efficiency η_{nom}, and the relative output λ_{in} which is calculated from the energy outflow $\dot{E}_{out}$ and the nominal capacitiy. Figure 1 shows the original input-output relationship, the linearization by Sass et al. (2020), and our linearization (relinearization).

2 Optimization models

In general, all components are modeled according to the description by Sass et al. (2020). The relevant differences between our study and Sass et al. (2020) are: (i) the removal of the electricity grid connection, (ii) our parameters for the linearized performance curves (cf. Section 1), and (iii) the utilized represen-

*M. Dahmen, Institute of Climate and Energy Systems, Energy Systems Engineering (ICE-1), Forschungszentrum Jülich GmbH, Jülich 52425, Germany
E-mail: m.dahmen@fz-juelich.de

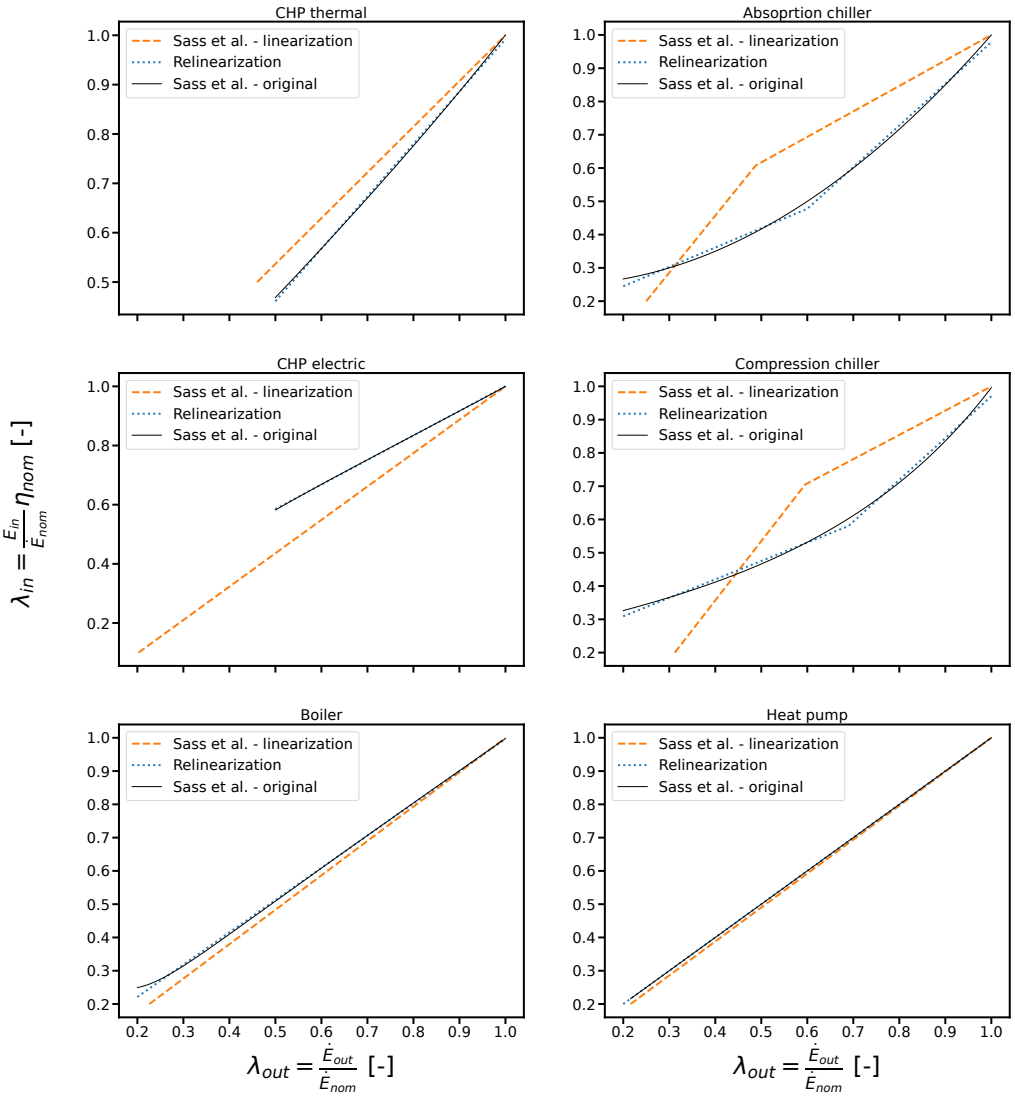

Fig. 1. Original input-output relationship according to Sass et al. (2020), linearization by Sass et al. (2020), and our linearization (relinearization).

Component	$\lambda_{in,0}$	$\lambda_{out,0}$	$\lambda_{in,1}$	$\lambda_{out,1}$	$\lambda_{in,2}$	$\lambda_{out,2}$
Boiler	0.221	0.2	0.996	1	-	-
CHP thermal	0.585	0.5	1	1	-	-
CHP electric	0.461	0.5	0.992	1	-	-
Absorption chiller (AC)	0.245	0.2	0.478	0.6	0.978	1
Compression chiller (CC)	0.309	0.2	0.580	0.689	0.97	1
Heat pump (HP)	0.2	0.2	1	1	-	-

Tab. 1. Linearization parameters for all conversion components.

tative scenario data and extreme scenarios, which are determined according to the description in Section 3 of the main manuscript.

Throughout the manuscript, scalar-valued quantities are denoted in regular font, e.g., x, vector-valued quantities are denoted in bold font, e.g., $\mathbf{x}$, and set-valued quantities are denoted in calligraphic font, e.g., $\mathcal{X}$.

$$\min_{\mathbf{x},\mathbf{z}} \sum_{c\in\mathcal{C}} \left(Capex_c \left(\frac{1}{\gamma_{pvf}} + \gamma_{maintenance,c} \right) \right) + \sum_{c\in\mathcal{C}_{fuel}} \sum_{s\in\mathcal{S}} \omega_s \sum_{t\in\mathcal{T}} \left(\gamma_{fuel} \dot{E}_{fuel,c,s,t} \Delta_t \right)$$

s.t. $\dot{E}_{e,dem,s,t} - \sum_{c\in\mathcal{C}_{e,out}} \dot{E}_{e,c,s,t} + \sum_{c\in\mathcal{C}_{e,in}} \dot{E}_{e,c,s,t} + \sum_{c\in\mathcal{C}_{e,sto}} \left(\dot{E}_{e,c,s,t,in} - \dot{E}_{e,c,s,t,out} \right) \leq 0 \qquad \forall e \in \mathcal{E}, \forall s \in \mathcal{S}, \forall t \in \mathcal{T}$

$\dot{E}_{nom,c} b_{ex,c} \leq \dot{E}_{max,c} \qquad \forall c \in \mathcal{C}$

$\dot{E}_{nom,c} b_{ex,c} \geq \dot{E}_{min,c} \qquad \forall c \in \mathcal{C}$

$Capex_c = \sum_{j\in\mathcal{J}_{capex,c}} b_{capex,c,j} Capex_{c,lb,j} + \beta_{capex,c,j} \left(\dot{E}_{nom,c,j} - \dot{E}_{lb,c,j} b_{capex,c,j} \right) \qquad \forall c \in \mathcal{C}$

$\dot{E}_{nom,c} = \sum_{j\in\mathcal{J}_{capex,c}} \dot{E}_{nom,c,j} \qquad \forall c \in \mathcal{C}$

$\dot{E}_{nom,c,j} b_{capex,c,j} \leq \dot{E}_{lb,c,j+1} \qquad \forall c \in \mathcal{C}, \forall j \in \mathcal{J}_{capex,c}$

$\dot{E}_{nom,c,j} b_{capex,c,j} \geq \dot{E}_{lb,c,j} \qquad \forall c \in \mathcal{C}, \forall j \in \mathcal{J}_{capex,c}$

$\sum_{j\in\mathcal{J}_{capex,c}} b_{capex,c,j} \leq 1 \qquad \forall c \in \mathcal{C}$

$$\dot{E}_{e_{in}(c),c,s,t} = \sum_{j\in\mathcal{J}_{eff,c}} b_{eff,e,c,s,t,j} \lambda_{in,e,c,j} \frac{\dot{E}_{nom,c}}{\eta_{nom,c,s,t}} + \frac{\beta_{eff,e,c,j}}{\eta_{nom,c,s,t}} \left(\dot{E}_{e,c,s,t,j} - \lambda_{out,e,c,j} b_{eff,e,c,s,t,j} \dot{E}_{nom,c} \right) \qquad \forall c \in \mathcal{C}_{conv}, \forall e \in \mathcal{E}_{out}(c), \forall s \in \mathcal{S}, \forall t \in \mathcal{T}$$

$\dot{E}_{e,c,s,t} = \sum_{j\in\mathcal{J}_{eff,c}} \dot{E}_{e,c,s,t,j} \qquad \forall c \in \mathcal{C}_{conv}, \forall e \in \mathcal{E}_{out}(c), \forall s \in \mathcal{S}, \forall t \in \mathcal{T}$

$\lambda_{out,e,c,j} \dot{E}_{nom,c} b_{eff,e,c,s,t,j} \leq \dot{E}_{e,c,s,t,j} \qquad \forall c \in \mathcal{C}_{conv}, \forall j \in \mathcal{J}_{eff,c}, \forall e \in \mathcal{E}_{out}(c), \forall s \in \mathcal{S}, \forall t \in \mathcal{T}$

$\lambda_{out,e,c,j+1} \dot{E}_{nom,c} b_{eff,e,c,s,t,j} \geq \dot{E}_{e,c,s,t,j} \qquad \forall c \in \mathcal{C}_{conv}, \forall j \in \mathcal{J}_{eff,c}, \forall e \in \mathcal{E}_{out}(c), \forall s \in \mathcal{S}, \forall t \in \mathcal{T}$

$\sum_{j\in\mathcal{J}_{eff,c}} b_{eff,e,c,s,t,j} \leq 1 \qquad \forall c \in \mathcal{C}_{conv}, \forall e \in \mathcal{E}_{out}(c), \forall s \in \mathcal{S}, \forall t \in \mathcal{T}$

$E_{e(c),c,s,t} \leq \gamma_{sto,c} \dot{E}_{nom,c} \qquad \forall c \in \mathcal{C}_{sto}, \forall s \in \mathcal{S}, \forall t \in \mathcal{T}$

$\dot{E}_{e(c),c,s,t,in} \leq \dot{E}_{nom,c} \qquad \forall c \in \mathcal{C}_{sto}, \forall s \in \mathcal{S}, \forall t \in \mathcal{T}$

$\dot{E}_{e(c),c,s,t,out} \leq \dot{E}_{nom,c} \qquad \forall c \in \mathcal{C}_{sto}, \forall s \in \mathcal{S}, \forall t \in \mathcal{T}$

$E_{e(c),c,s,t} \left(1 + \frac{\Delta_t}{\tau_c} \right) = E_{e(c),c,s,t-1} + \Delta_t \left(\eta_{c,in} \dot{E}_{e(c),c,s,t,in} - \frac{\dot{E}_{e(c),c,s,t,out}}{\eta_{c,out}} \right) \qquad \forall c \in \mathcal{C}_{sto}, \forall s \in \mathcal{S}, \forall t \in \mathcal{T} \setminus \{1\}$

$E_{e(c),c,s,1} \left(1 + \frac{\Delta_t}{\tau_c} \right) = E_{e(c),c,s,|\mathcal{T}|} + \Delta_t \left(\eta_{c,in} \dot{E}_{e(c),c,s,1,in} - \frac{\dot{E}_{e(c),c,s,1,out}}{\eta_{c,out}} \right) \qquad \forall c \in \mathcal{C}_{sto}, \forall s \in \mathcal{S}$

$E_{e(c),c,s,1} = E_{init,c} \qquad \forall c \in \mathcal{C}_{sto}, \forall s \in \mathcal{S}$

$\dot{E}_{e(c),c,s,t} \leq f_{solar,s,t} \dot{E}_{nom,c} \qquad \forall c \in \{PV_i \mid \forall i \in 1, \ldots, n_{components}\}, \forall s \in \mathcal{S}, \forall t \in \mathcal{T}$

with

$$\mathbf{x} = [\underbrace{Capex_c, \dot{E}_{nom,c}, b_{ex,c}}_{\forall c \in \mathcal{C}}, \underbrace{E_{init,c}}_{\forall c \in \mathcal{C}_{sto}}, \underbrace{\dot{E}_{nom,c,j}, b_{capex,c,j}}_{\forall c \in \mathcal{C}, \forall j \in \mathcal{J}_{capex,c}}]$$

$$Capex_c \in \mathbb{R}_{\geq 0}, \dot{E}_{nom,c} \in \mathbb{R}_{\geq 0}, b_{ex,c} \in \{0,1\}$$

$$\mathbf{z} = [\underbrace{\dot{E}_{e,c,s,t}}_{\forall c \in \mathcal{C}_{conv}, \forall e \in \mathcal{E}(c), \forall s \in \mathcal{S}, \forall t \in \mathcal{T}}, \underbrace{\dot{E}_{e,c,s,t,in}, \dot{E}_{e,c,s,t,out}}_{\forall c \in \mathcal{C}_{sto}, \forall e \in \mathcal{E}(c), \forall s \in \mathcal{S}, \forall t \in \mathcal{T}}, \underbrace{E_{e(c),c,s,t}}_{\forall c \in \mathcal{C}_{sto}, \forall s \in \mathcal{S}, \forall t \in \mathcal{T}}, \underbrace{\dot{E}_{e,c,s,t,j}, b_{eff,e,c,s,t,j}}_{\forall c \in \mathcal{C}_{conv}, \forall e \in \mathcal{E}_{out}(c), \forall s \in \mathcal{S}, \forall t \in \mathcal{T}, \forall j \in \mathcal{J}_{eff,c}}]$$

$$\dot{E}_{e,c,s,t} \in \mathbb{R}_{\geq 0}, \dot{E}_{e,c,s,t,j} \in \mathbb{R}_{\geq 0}, \dot{E}_{e,c,s,t,in} \in \mathbb{R}_{\geq 0}, \dot{E}_{e,c,s,t,out} \in \mathbb{R}_{\geq 0}, E_{e(c),c,s,t} \in \mathbb{R}_{\geq 0}, b_{eff,e,c,s,t,j} \in \{0,1\}$$

$$\mathcal{C} = \{CHP_{small,i}, CHP_{medium,i}, CHP_{large,i}, Boiler_i, CC_i, AC_i, HP_i, PV_i, Battery_i,$$
$$TES_{heat,i}, TES_{cooling,i} \mid i = 1, \ldots, n_{components}\}$$

$$\mathcal{C}_{fuel} = \{CHP_{small,i}, CHP_{medium,i}, CHP_{large,i}, Boiler_i \mid i = 1, \ldots, n_{components}\}$$

$$\mathcal{C}_{conv} = \{CHP_{small,i}, CHP_{medium,i}, CHP_{large,i}, Boiler_i, CC_i, AC_i, HP_i \mid i = 1, \ldots, n_{components}\}$$

$$\mathcal{C}_{sto} = \{Battery_i, TES_{heat,i}, TES_{cooling,i} \mid i = 1, \ldots, n_{components}\}$$

$$\mathcal{C}_{heat,out} = \{CHP_{small,i}, CHP_{medium,i}, CHP_{large,i}, Boiler_i, HP_i \mid i = 1, \ldots, n_{components}\}$$

$$\mathcal{C}_{heat,in} = \{AC_i \mid i = 1, \ldots, n_{components}\}$$

$$\mathcal{C}_{electricity,out} = \{CHP_{small,i}, CHP_{medium,i}, CHP_{large,i} \mid i = 1, \ldots, n_{components}\}$$

$$\mathcal{C}_{electricity,in} = \{CC_i, HP_i \mid i = 1, \ldots, n_{components}\}$$

$$\mathcal{C}_{cooling,out} = \{CC_i, AC_i \mid i = 1, \ldots, n_{components}\}$$

$$\mathcal{E} = \{heat, electricity, cooling\}$$

Here, $\mathbf{x}$ are the design variables and $\mathbf{z}$ are the operational variables. The considered components are boilers, three different sizes of CHPs (small, medium, large), absorption chillers (ACs), compression chillers (CCs), heat pumps (HPs), photovoltaic modules (PVs), batteries, and thermal energy storage (TES) for heat and cooling. $Capex_c$ are the capital expenditures to install component c, $\dot{E}_{fuel,c,s,t}$ are the energy imports of fuel, i.e., natural gas, for the fuel burning components, which are boilers and CHPs. In our example, up to $n_{components} = 2$ copies can be installed of each component.

$\mathcal{E}$ is the set of energy forms, $\mathcal{S}$ is the set of scenarios and $\mathcal{T}$ is the set of timesteps. $\mathcal{J}_{capex,c}$ is the set of linearization indices for the linearization of the capital expenditures for each component, and $\mathcal{J}_{eff,c}$ is the set of linearization indices for the linearization of the energy inflow-outflow relationship for each component. $\mathcal{C}$ is the set of components, $\mathcal{C}_{fuel}$ is the set of components supplied externally by gas, $\mathcal{C}_{conv}$ is

the set of conversion components, $\mathcal{C}_{sto}$ is the set of storage components, $\mathcal{C}_{heat,out}$ and $\mathcal{C}_{heat,in}$ are the sets of components whose energy outflows and inflows are heat, respectively. $\mathcal{C}_{electricity,out}$ and $\mathcal{C}_{electricity,in}$ are the sets of components whose energy outflows and inflows are electricity, respectively, and $\mathcal{C}_{cooling,out}$ is the set of components whose energy outflows are cooling and there are no conversion components taking cooling energy as input. $e_{in}(c)$ is a function that maps each component to its inflow energy, and $e(c)$ maps each storage component to its inflow and outflow energy. A similar mapping cannot be constructed for the energy outflows, as the CHPs have two output energy forms.

$\dot{E}_{e,c,s,t}$ are the energy flows of energy form e for conversion component c in scenario s and timestep t, while $\dot{E}_{e,c,s,t,in}$ and $\dot{E}_{e,c,s,t,out}$ are the energy inflows and outflows of storage components, and $E_{init,c}$ is the initial state of charge. In the default case study, the initial state of charge is fixed to 50% of the nominal capacity; in the variable SOC case study, it is a design variable. $\dot{E}_{nom,c}$ is the nominal capacity of component c and $b_{ex,c}$ is a binary variable that indicates whether component c has been installed.

The nonlinear dependency of $Capex_c$ on $\dot{E}_{nom,c}$ is approximated by a piecewise-linear relationship. To this end, binary variables $b_{capex,c,j}$ indicate which segment $j \in \mathcal{J}_{capex,c}$ of the piecewise linearization is active. $\dot{E}_{nom,c,j}$ is the nominal capacity variable for each respective segment. Similarly, the nonlinear dependency of $\dot{E}_{e_{in}(c),c,s,t}$ on $\dot{E}_{e,c,s,t}$ is approximated by a piecewise-linear relationship. Importantly, for the CHPs, there are two output energy forms, electricity and heat. Hence, $\mathcal{E}_{out}(c)$ are the index sets that contain all output energy forms for each component. Again, $b_{eff,e,c,s,t,j}$ are binary variables that indicate which segment $j \in \mathcal{J}_{eff,c}$ of the linearization is active, and $\dot{E}_{e,c,s,t,j}$ is the output energy flow for that segment. $E_{e(c),c,s,t}$ are the storage levels of each storage. The equation to determine the energy storage level is obtained by using the implicit Euler scheme on the differential equation of the storage. For a detailed description of the linearization formulation and the modeling equations, we refer to Sass et al. (2020). Note that where Sass et al. (2020) use Q to refer to energy flow, we use $\dot{E}$.

The energy flow demands $\dot{E}_{e,dem,s,t}$, the capacity factor of the PV modules $f_{solar,s,t}$, and the ambient temperature $T_{amb,s,t}$ are uncertain variables that are determined for each representative scenario s from historical data. The ambient temperature is then used to calculate the efficiency of the heat pumps: $\eta_{nom,HP_i,s,t}(T_{amb,s,t}) = \frac{0.36 T_{hp}}{T_{hp} - T_{amb,s,t}}$. For all other components, the nominal efficiency $\eta_{nom,c,s,t}$ is constant and does not depend on uncertain variables.

The objective function minimizes the total annualized cost. To this end, the present value factor is defined as

$$\gamma_{pvf} = \frac{(1+0.08)^4 - 1}{0.08\,(1+0.08)^4}$$

for an interest rate of 0.08 and a time horizon of 4 years. The maintenance factors $\gamma_{maintenance,c}$ can be

obtained from Tables 1 and 2 in Sass et al. (2020). The scenario weights are defined as

$$\omega_s = 365 \frac{n_{data,s}}{n_{data}},$$

where $n_{data,s}$ are the number of days in the historical data in the cluster of scenario s and n_{data} are the total number of days in the historical data. $\gamma_{fuel} = 0.08 \frac{\text{EUR}}{\text{kWh}}$ are the fuel costs and Δ_t is the timestep length, which is 2 h in our example.

The parameters for the economic variables $Capex_{c,lb,j}$ and the capacities $\dot{E}_{lb,c,j}$ can be obtained from Sass et al. (2020) in their publication from Table C.2. Note, that we use $\dot{E}_{lb,c,j}$ where Sass et al. (2020) use $Q^{lb}_{i,j}$, $\dot{E}_{max,c}$ and $\dot{E}_{min,c}$ correspond to the smallest and largest values of $\dot{E}_{lb,c,j}$. $\beta_{capex,c,j}$ is calculated as

$$\beta_{capex,c,j} = \frac{Capex_{c,lb,j+1} - Capex_{c,lb,j}}{\dot{E}_{lb,c,j+1} - \dot{E}_{lb,c,j}}.$$

The values for the linearization parameters $\lambda_{in,e,c,j}$ and $\lambda_{out,e,c,j}$ of the piecewise-linear energy inflow-outflow curves can be found in Section 1. $\beta_{eff,e,c,j}$ is calculated as

$$\beta_{eff,e,c,j} = \frac{\lambda_{in,e,c,j+1} - \lambda_{in,e,c,j}}{\lambda_{out,e,c,j+1} - \lambda_{out,e,c,j}}.$$

$\gamma_{sto,c}$ is the coefficient that determines the relation between the nominal capacity of each storage component to the maximum storage capacity. For batteries it is 4 $\frac{\text{kWh}}{\text{kW}}$ and for thermal energy storages 1 $\frac{\text{kWh}}{\text{kW}}$. While τ_c are the time constants for self-discharge, and $\eta_{c,in}$ and $\eta_{c,out}$ are the charging and discharging efficiencies.

The operational problem is formulated as:

$$\min_{\mathbf{z},\phi} \ \phi$$

$$\text{s.t.} \quad \dot{E}_{e,dem,t} - \sum_{c\in\mathcal{C}_{e,out}} \dot{E}_{e,c,t} + \sum_{c\in\mathcal{C}_{e,in}} \dot{E}_{e,c,t} + \sum_{c\in\mathcal{C}_{e,sto}} \left(\dot{E}_{e,c,t,in} - \dot{E}_{e,c,t,out}\right) \leq \phi \qquad \forall e\in\mathcal{E}, \forall t\in\mathcal{T}$$

$$\dot{E}_{e_{in}(c),c,t} = \sum_{j\in\mathcal{J}_{eff,c}} b_{eff,e,c,t,j}\lambda_{in,e,c,j}\frac{\dot{E}_{nom,c}}{\eta_{nom,c,t}}$$

$$+ \frac{\beta_{eff,e,c,j}}{\eta_{nom,c,t}}\left(\dot{E}_{e,c,t,j} - \lambda_{out,e,c,j}b_{eff,e,c,t,j}\dot{E}_{nom,c}\right) \qquad \forall c\in\mathcal{C}_{conv}, \forall e\in\mathcal{E}_{out}(c), \forall t\in\mathcal{T}$$

$$\dot{E}_{e,c,t} = \sum_{j\in\mathcal{J}_{eff,c}} \dot{E}_{e,c,t,j} \qquad \forall c\in\mathcal{C}_{conv}, \forall e\in\mathcal{E}_{out}(c), \forall t\in\mathcal{T}$$

$$\lambda_{out,e,c,j}\dot{E}_{nom,c}b_{eff,e,c,t,j} \leq \dot{E}_{e,c,t,j} \qquad \forall c\in\mathcal{C}_{conv}, \forall j\in\mathcal{J}_{eff,c}, \forall e\in\mathcal{E}_{out}(c), \forall t\in\mathcal{T}$$

$$\lambda_{out,e,c,j+1}\dot{E}_{nom,c}b_{eff,e,c,t,j} \geq \dot{E}_{e,c,t,j} \qquad \forall c\in\mathcal{C}_{conv}, \forall j\in\mathcal{J}_{eff,c}, \forall e\in\mathcal{E}_{out}(c), \forall t\in\mathcal{T}$$

$$\sum_{j\in\mathcal{J}_{eff,c}} b_{eff,e,c,t,j} \leq 1 \qquad \forall c\in\mathcal{C}_{conv}, \forall e\in\mathcal{E}_{out}(c), \forall t\in\mathcal{T}$$

$$E_{e(c),c,t} \leq \gamma_{sto,c}\dot{E}_{nom,c} \qquad \forall c\in\mathcal{C}_{sto}, \forall t\in\mathcal{T}$$

$$\dot{E}_{e(c),c,t,in} \leq \dot{E}_{nom,c} \qquad \forall c\in\mathcal{C}_{sto}, \forall t\in\mathcal{T}$$

$$\dot{E}_{e(c),c,t,out} \leq \dot{E}_{nom,c} \qquad \forall c\in\mathcal{C}_{sto}, \forall t\in\mathcal{T}$$

$$E_{e(c),c,t}\left(1+\frac{\Delta_t}{\tau_c}\right) = E_{e(c),c,t-1} + \Delta_t\left(\eta_{c,in}\dot{E}_{e(c),c,t,in} - \frac{1}{\eta_{c,out}}\dot{E}_{e(c),c,t,out}\right) \qquad \forall c\in\mathcal{C}_{sto}, \forall t\in\mathcal{T}\setminus\{1\}$$

$$E_{e(c),c,1}\left(1+\frac{\Delta_t}{\tau_c}\right) = E_{e(c),c,|\mathcal{T}|} + \Delta_t\left(\eta_{c,in}\dot{E}_{e(c),c,1,in} - \frac{1}{\eta_{c,out}}\dot{E}_{e(c),c,1,out}\right) \qquad \forall c\in\mathcal{C}_{sto}$$

$$E_{e(c),c,1} = E_{init,c} \qquad \forall c\in\mathcal{C}_{sto}$$

$$\dot{E}_{e(c),c,t} \leq f_{solar,t}\dot{E}_{nom,c} \qquad \forall c\in\{PV_i \mid \forall i\in 1,\ldots,n_{components}\}, \forall s\in\mathcal{S}, \forall t\in\mathcal{T}$$

with

$$\mathbf{z} = [\ \underbrace{\dot{E}_{e,c,t}}_{\forall c\in\mathcal{C}_{conv},\forall e\in\mathcal{E}(c),\forall t\in\mathcal{T}}, \underbrace{\dot{E}_{e,c,t,in}, \dot{E}_{e,c,t,out}}_{\forall c\in\mathcal{C}_{sto},\forall e\in\mathcal{E}(c),\forall t\in\mathcal{T}}, \underbrace{E_{e(c),c,t}}_{\forall c\in\mathcal{C}_{sto},\forall t\in\mathcal{T}}, \underbrace{\dot{E}_{e,c,t,j}, b_{eff,e,c,t,j}}_{\forall c\in\mathcal{C}_{conv},\forall e\in\mathcal{E}_{out}(c),\forall t\in\mathcal{T},\forall j\in\mathcal{J}_{eff,c}}\ ]$$

$$\phi\in\mathbb{R}, \dot{E}_{e,c,t}\in\mathbb{R}_{\geq 0}, \dot{E}_{e,c,t,j}\in\mathbb{R}_{\geq 0}, \dot{E}_{e,c,t,in}\in\mathbb{R}_{\geq 0}, \dot{E}_{e,c,t,out}\in\mathbb{R}_{\geq 0}, E_{e(c),c,t}\in\mathbb{R}_{\geq 0}, b_{eff,e,c,t,j}\in\{0,1\}$$

The operational problem is similar to the design problem. The equations to calculate the capital expenditures are omitted, and the objective function is replaced by an auxiliary variable ϕ, which measures

the maximum violation of the energy balance equations. Variables and parameters are similar to the design problem, except that no scenario index is included, as there is only one scenario per operational problem.

References

Sass, S., Faulwasser, T., Hollermann, D. E., Kappatou, C. D., Sauer, D., Schütz, T., Shu, D. Y., Bardow, A., Gröll, L., Hagenmeyer, V., Müller, D., and Mitsos, A. (2020). Model compendium, data, and optimization benchmarks for sector-coupled energy systems. *Computers & Chemical Engineering*, 135:106760.